# Formation of huge cyclic oligomers in the condensation polymerization of bis(9-hydroxy-1,4,7-trioxanonyl) substituted naphthalene and benzenes with both aromatic and aliphatic bis-acid chlorides

**Ingrid J. A. Mertens,[a] René Wegh,[a] Leonardus W. Jenneskens,*[,a] Edward J. Vlietstra,[a] Anca van der Kerk-van Hoof,[b] Jan W. Zwikker,[a] Thomas J. Cleij,[a] Wilberth J. J. Smeets,[c] Nora Veldman[c] and Anthony L. Spek[c]**

[a] *Debye Institute, Department of Physical Organic Chemistry, Utrecht University, Padualaan 8, 3584 CH Utrecht, The Netherlands*
[b] *Bijvoet Center for Biomolecular Research, Department of Mass Spectrometry, Utrecht University, PO Box 80083, 3508 TB Utrecht, The Netherlands*
[c] *Bijvoet Center for Biomolecular Research, Department of Crystal- and Structural Chemistry, Utrecht University, Padualaan 8, 3584 CH Utrecht, The Netherlands*



**Without the use of high dilution techniques condensation polymerization of bis(9-hydroxy-1,4,7-trioxanonyl) substituted naphthalene and benzenes (1a–d) with the bis-acid chlorides terephthaloyl dichloride (2), adipoyl dichloride (5a) and isophthaloyl dichloride (5b) at 80 °C, respectively, gives giant-size macrocycles, *i.e.* crownophanes 3a(*n*) with *n* = 1–5, 3b–d(*n*) with *n* = 1–3 and 6a–b(*n*) with *n* = 1–2, respectively, in high overall yield (*ca.* 30% w/w, monomer conc. 0.033 M). The crownophanes with 28–150 atom perimeters have been isolated using preparative column chromatography. Both in the melt and in solution, with a ten-fold increase in monomer conc. (0.33 M), cyclic oligomer yields remain considerable (melt, *ca.* 2% w/w, and solution *ca.* 10% w/w). $^1$H NMR conformational analysis of the 9-hydroxy-1,4,7-trioxanonyl side chains of both 1a and 1d at 25 and 80 °C have shown that all HO–[CH(I)$_2$–CH(II)$_2$–O]$_n$– units are almost exclusively present in their *gauche* conformation at both temperatures. This is supported by semi-empirical AM1 calculations. Hence, favourable pre-orientation of the side chains is apparently an important factor in the formation of cyclic oligomers. Single crystal X-ray structures of 3a(1), 3d(1) and 6a(1) are reported; solid-state packing motifs are strongly affected by the type of diol and bis-acid constituent.**

## Introduction

Although it is well established that during condensation polymerizations,[1] in addition to formation of linear polymers, cyclic oligomers are generated as side products,[2] under common conditions (ratio diol : bis-acid 1 : 1, either in the melt or in solution) the cyclic oligomer yield is invariably low (*ca.* 1–5% w/w). Consequently, only a small number of cyclic oligomers have been isolated and characterized. This is unfortunate since they can be used to assess differences as well as similarities between cyclic and linear oligomers *versus* the polymer. Furthermore, if ligating sites such as HO–[CH(I)$_2$–CH(II)$_2$–O]$_n$– units are present, cyclic oligomers serve as model systems to mimic natural compounds such as ionophores.[3] To obtain large cyclic oligomers, the most widely used method is the high dilution technique, *i.e.* condensation reactions are carried out under high dilution conditions.[4] Although this reduces the probability of polymerization, cyclic oligomer yields in general remain low (*ca.* 15% w/w).[5] Other approaches are the use of (self)-organization through molecular recognition of reactants, the application of multiple cycloadditions and *via* immobilization of the reactants on solid substrates.[6–8]

In a recent communication we have reported on the formation of huge macrocyclics, *i.e.* crownophanes[9] **3a**(*n*) with *n* = 1–5, during condensation polymerization of 1,5-bis(9-hydroxy-1,4,7-trioxanonyl)naphthalene (**1a**) with terephthaloyl dichloride (**2**).[10] Both in the melt and in solution (monomer conc. either 0.33 or 0.033 M), a homologous series of cyclic oligomers **3a**(*n*) is formed in addition to the linear polymer **4a** in considerable amounts (2, 10 and 30% w/w for melt, 0.33 and 0.033 M, respectively, Scheme 1, *vide infra*). It should be stipulated that no high dilution conditions[4] were applied! The work presented in this paper was initiated to elucidate the following issues. (*i*) To what extent is cyclic oligomer formation during condensation polymerization of bis(9-hydroxy-1,4,7-trioxanonyl) substituted aromatics **1a–d** with the bis-acid chlorides terephthaloyl dichloride (**2**), adipoyl dichloride (**5a**) and isophthaloyl dichloride (**5b**), affected by the structural flexibility and topology of the diols as well as the bis-acid chlorides? (*ii*) What are the factors responsible for the cyclic oligomer formation?

## Results and discussion

### Formation and isolation of cyclic oligomers

Condensation polymerization was performed with 1,5-bis(9-hydroxy-1,4,7-trioxanonyl)naphthalene (**1a**) and *ortho*, *meta* and *para* bis(9-hydroxy-1,4,7-trioxanonyl) substituted benzenes, *viz*. 1,2-bis(9-hydroxy-1,4,7-trioxanonyl)benzene (**1b**), 1,3-bis(9-hydroxy-1,4,7-trioxanonyl)benzene (**1c**) and 1,4-bis(9-hydroxy-1,4,7-trioxanonyl)benzene (**1d**), respectively, with terephthaloyl dichloride (**2**, Scheme 1, monomer conc. 0.033 M). Evidence for the formation of a distinct series of cyclic oligomers was obtained from an analysis of the crude reaction mixtures of **1a–d/2**, using thin layer chromatography (TLC) and gel permeation chromatography (GPC). TLC revealed the presence of at least three low molecular weight components, which migrated, in contrast to the high molecular weight material. Precipitation of the high molecular weight fraction of **1a–d/2** in a five-fold excess of methanol followed by GPC analysis of both the vis-

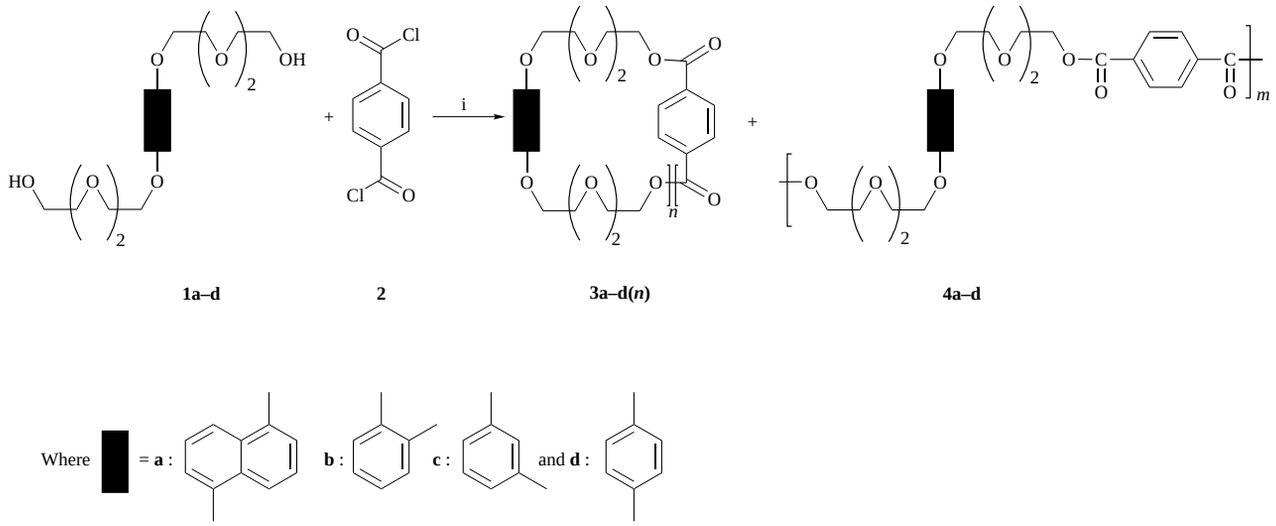


**Scheme 1** *Reagents and conditions*: i, 1,2-dichloroethane, pyridine, reflux



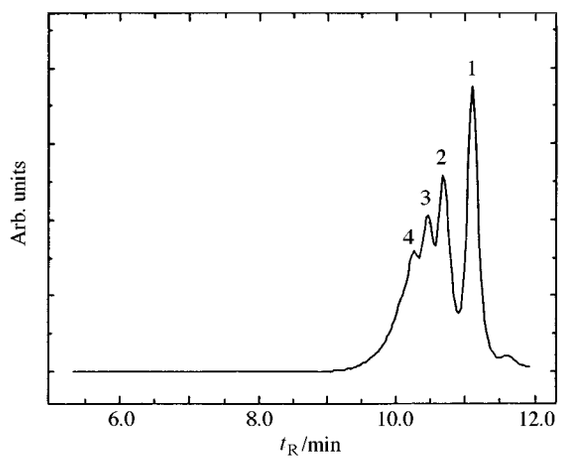


**Fig. 1** GPC trace of the low molecular weight fraction containing **3a**(*n*) with *n* = 1–5

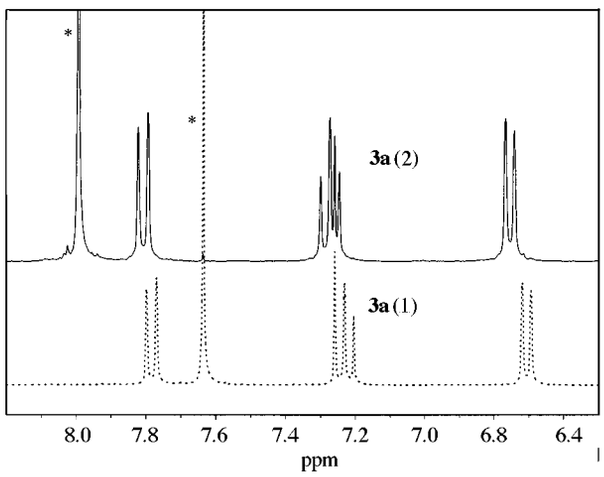


**Fig. 2** Aromatic part of the $^1$H NMR spectra of **3a**(1) and **3a**(2) [* terephthaloyl protons]

cous precipitate and the methanol-soluble fraction, showed that the low molecular weight compounds are soluble in methanol; in the case of the methanol-soluble fraction of **1a/2** at least four major products were observed (Fig. 1). Furthermore, the GPC retention times [$t_R$(GPC)] found within each series suggest that the low molecular weight compounds are structurally related. On the basis of the polystyrene calibration curve, consecutive mass increments of *ca*. 550 [**3a**(*n*)] and 500 [**3b**–**d**(*n*)] amu concomitant with increasing *n* were found. For their preparative isolation a two step column chromatography (silica gel; eluent acetone–*n*-hexane 1 : 1 v/v) procedure was used in the case of **3a**(*n*). While **3a**(1) and **3a**(2) could be isolated directly from the concentrated methanol-soluble fraction, **3a**(3–5) were obtained as a mixture. The latter were separated in a second preparative column chromatography run (silica gel; eluent acetone–*n*-hexane 1 : 1 v/v). Compounds **3b**(1–3), **3c**(1,2) and **3d**(1–3) were isolated in a single preparative column chromatography (silica gel; eluent acetone–*n*-hexane 1 : 1 v/v) run. High-performance liquid column chromatography (HPLC) showed that the isolated compounds within each series possess different retention times [$t_R$(HPLC)] and purities exceeding 95% (Tables 1 and 2). Note that the isolated yields for **3b**–**d**(*n*) with *n* = 1–3 were higher than those of **3a**(*n*) with *n* = 1–5. However, HPLC analysis of the crude low molecular weight fractions revealed that the amount of cyclic oligomers obtained during each condensation polymerization is nearly identical in every series. Therefore, we conclude that the preparative column chromatography procedure applied for the isolation of compounds **3a**(*n*) is apparently not as effective as in the case of **3b**–**d**(*n*). However, the simplicity of the isolation procedure and its suitability for scaling up enables the isolation of **3a**(*n*) with *n* = 1–5 in reasonable amounts.

### Characterization of cyclic oligomers

It should be stipulated that within each series the elemental composition of the cyclic oligomers is identical, since they all consist of *n* times the diol and the bis-acid moiety in a 1 : 1 ratio. Indeed, $^1$H NMR spectroscopy unequivocally showed that all the isolated compounds consist of coupled monomers in a 1 : 1 ratio. Neither hydroxy nor carboxylate endgroups were discernible ($^1$H NMR and FTIR spectroscopy). $^1$H NMR and $^{13}$C NMR spectroscopy revealed that all spectra within each series are virtually identical with the exception of the $^1$H NMR spectra of **3a**–**d**(1). For example, in the case of **3a**(1) an upfield shift for the terephthaloyl protons ($\Delta\delta$ −0.40)[10] is observed, which is not discernible in the $^1$H NMR spectra of **3a**(*n*) with $n \geqslant 2$ (Fig. 2).† This suggests that in solution the terephthaloyl protons of **3a**(1) are positioned in the shielding cone region of the bis-substituted naphthalene moiety (see single crystal X-ray structure determinations). These spectroscopic data strongly indicate that the isolated compounds are cyclic oligomers with increasing values of *n*. This is corroborated by FABMS; con-

† In the case of **3b**–**d**(1) no clear shielding cone effects are discernible; only moderate upfield shifts (*ca*. $\Delta\delta$ −0.03) are found.

**Table 1** Salient features of cyclic oligomers **3a**(*n*)[10]

| Ring | Size[a] | $t_R$(GPC)/ min | $t_R$(HPLC)/ min | Yield (HPLC) (% w/w) | Isolated yield [% w/w (purity)] | FABMS ([M+H]$^+$) | DSC $T_m$ ($T_g$)[b]/ °C |
|---|---|---|---|---|---|---|---|
| **3a**(1) | 30 | 11.13 | 5.31 | 21.9 | 10.3 (>99%) | 555 | 116.7[c] |
| **3a**(2) | 60 | 10.71 | 9.82 | 4.7 | 3.2 (>99%) | 1109 | 125.0[c] |
| **3a**(3) | 90 | 10.48 | 11.80 | 1.0 | 1.2 (>99%) | 1663 | (0.5) |
| **3a**(4) | 120 | 10.25 | 12.93 | 0.2 | 1.2 (>95%) | 2217 | (0.0) |
| **3a**(5) | 150 | 10.09 | 14.53 | 0.2 | 0.1 (>95%) | 2771 | — |

[a] Size represents the number of atoms determining the ring perimeter. [b] Melting points; peak maximum taken from the second heating run. Glass transition temperatures ($T_g$) are midpoint values. [c] For melt enthalpies $\Delta H$ in cal g$^{-1}$; see Experimental section.

**Table 2** Salient features of cyclic oligomers **3b**–**d**(*n*)

| Ring | Size[a] | $t_R$(GPC)/ min | $t_R$(HPLC)/ min | Isolated yield [% w/w (purity)] | FABMS [M+H]$^+$ | DSC $T_m$ ($T_g$)/ °C |
|---|---|---|---|---|---|---|
| **3b**(1) | 28 | 11.09 | 3.74 | 30 (>99%) | 505 | 80.7[b](−17.5)[c] |
| **3b**(2) | 56 | 10.65 | 6.96 | 5 (>99%) | 1009 | 111.1[b](−11.2)[c] |
| **3b**(3) | 84 | 10.42 | 9.08 | 1 (>95%) | 1513 | (−23.3) |
| **3c**(1) | 29 | 11.10 | 4.12 | 21 (>99%) | 505 | 98.6[b] |
| **3c**(2) | 58 | 10.69 | 7.47 | 3 (>96%) | 1009 | 74.2[b] (−7.2)[d] |
| **3c**(3) | 87 | 10.47 | 9.51 | *e* | 1513 | *f* |
| **3d**(1) | 30 | 11.08 | 3.76 | 23 (>99%) | 505 | 91.6[b] (−8.8)[c] |
| **3d**(2) | 60 | 10.80 | 7.15 | 4 (>98%) | 1009 | 115.3[b] |
| **3d**(3) | 90 | 10.44 | 9.11 | 1 (>95%) | 1513 | *f* |

[a] Size represents the number of atoms determining the ring perimeter. [b] For melt enthalpies $\Delta H$ in cal g$^{-1}$; see Experimental section. [c] No crystallization occurs during its cooling run; in the second heating run a glass transition [$T_g$ (midpoint value)] is found, followed by cold crystallization and again the melting process upon further heating. [d] No crystallization occurs during its cooling run; in the second heating run only a glass transition ($T_g$) is found. [e] Not isolated. [f] Not determined.

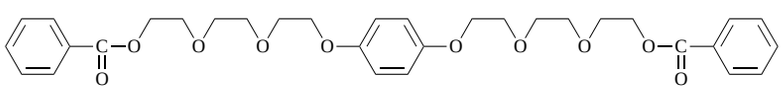

**8**

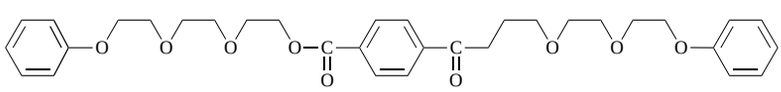

**9**

comitant with increasing *n* [M+H]$^+$ molecular ions are found which differ by consecutive 554 [**3a**(*n*)] and 504 [**3b**–**d**(*n*)] amu increments (Tables 1 and 2). A characteristic loss of (multiple) $C_2H_4O$ (44 amu) fragments directly from [M+H]$^+$ is found for macrocycles containing coupled ethylene glycol units.[11,12] Although the linear reference compounds **8** and **9** ([M+H]$^+$ = 583) also show loss of $C_2H_4O$ units, this never occurs directly from the molecular ion, *i.e.* no fragment ion with *m*/*z* 539 is found. Hence, huge cyclic oligomers are indeed obtained. For **3a**(1), **3d**(1) and **6a**(1) this is further supported by single crystal X-ray structure determinations (*vide infra*).

The thermal properties of the crownophanes were assessed using differential scanning calorimetry (DSC) and polarization microscopy. Whereas all compounds with $n = 1$ and 2 are crystalline solids, those with $n > 2$ only possess a glass transition. No (thermotropic) liquid crystalline behaviour was observed (Tables 1 and 2). To determine if intramolecular interactions between the incorporated bis-substituted naphthalene and phenyl moieties occur cyclic voltammetry measurements were made. For the bis-substituted naphthalene moiety in **1a** and **3a**(*n*) only an irreversible one-electron oxidation (anodic peak potential, $E_{pa}$ 1.05 V) was observed. In the case of the phenyl derivatives an irreversible one-electron oxidation was also found [$E_{pa}$, **1b** and **3b**(*n*) 1.41 V; **1c** and **3c**(*n*) 1.53 V; **1d** and **3d**(*n*) 1.19 V]. For all compounds an irreversible one-electron reduction wave ($E_{pc}$ −1.88 V) was obtained for the terephthaloyl unit, which corresponds to the $E_{pc}$ value (−1.85 V) of dimethyl terephthalate. Since within each series $E_{pa}$ and $E_{pc}$ values are essentially identical, no interactions between the redox-active moieties are discernible. This is supported by UV–VIS spectroscopy, *viz*. the spectra of the cyclic oligomers are identical to sum spectra obtained for equimolar mixtures of appropriate reference compounds such as **1a** and dimethyl terephthalate; no additional charge transfer[13] absorption bands are found.

### Cyclic oligomer yield

To determine whether the nature and the geometry of the bis-acid moiety affects the formation of cyclic oligomers, adipoyl dichloride (**5a**) and isophthaloyl dichloride (**5b**) were used as bis-acid chlorides in condensation polymerization reactions with diol **1a** (monomer conc. 0.033 M, Scheme 2). From the crude fractions containing low molecular weight material of **1a**/**5a** and **1a**/**5b** the cyclic oligomers **6a**(1,2) and **6b**(1,2), respectively, were readily isolated using the preparative column chromatography procedure (Table 3). Note, however, that no higher homologues, *viz*. **6a**(*n*) and **6b**(*n*) with $n > 2$, could be identified. Compared to the results obtained for polycondensation of **1a** and **2** under identical conditions, similar overall cyclic oligomer yields were found with both adipoyl dichloride (**5a**) and isophthaloyl dichloride (**5b**) (Tables 1 and 3).

Therefore, we subsequently investigated to what extent the overall cyclic oligomer yields are affected by the monomer concentration during polycondensation. Condensation polymeriz-

**Table 3** Salient features of cyclic oligomers **6a**(*n*) and **6b**(*n*)

| Ring | Size[a] | $t_R$(GPC)/ min | $t_R$(HPLC)/ min | Yield (HPLC) (% w/w) | FABMS $[M+H]^+$ | DSC $T_m$ ($T_g$)/ °C |
|---|---|---|---|---|---|---|
| **6a**(1)[b] | 32 | 11.16 | 4.39 | 16.4 | 535 | 100.7[c] |
| **6a**(2)[b] | 64 | 10.78 | 8.06 | 4.9 | 1069 | 52.5[c] (−18.4)[d] |
| **6b**(1)[b,e] | 29 | 11.03 | 6.42 | 19.5 | 555 | 82.2[c] (0.7)[d] |
| **6b**(2)[b,e] | 58 | 10.63 | 10.72 | 4.8 | 1109 | 120.5[c] (11.9)[d] |

[a] Size represents the number of atoms determining the ring perimeter. [b] Compounds **6a**,**b**(*n*) with $n = 1$ and 2 were isolated by preparative column chromatography. [c] For melt enthalpies $\Delta H$ in cal $g^{-1}$; see Experimental section. [d] No crystallization during its cooling run; in the second heating run only a glass transition ($T_g$) is found. [e] HPLC **6b**(*n*); elution velocity 0.8 ml $min^{-1}$ (see Experimental section).

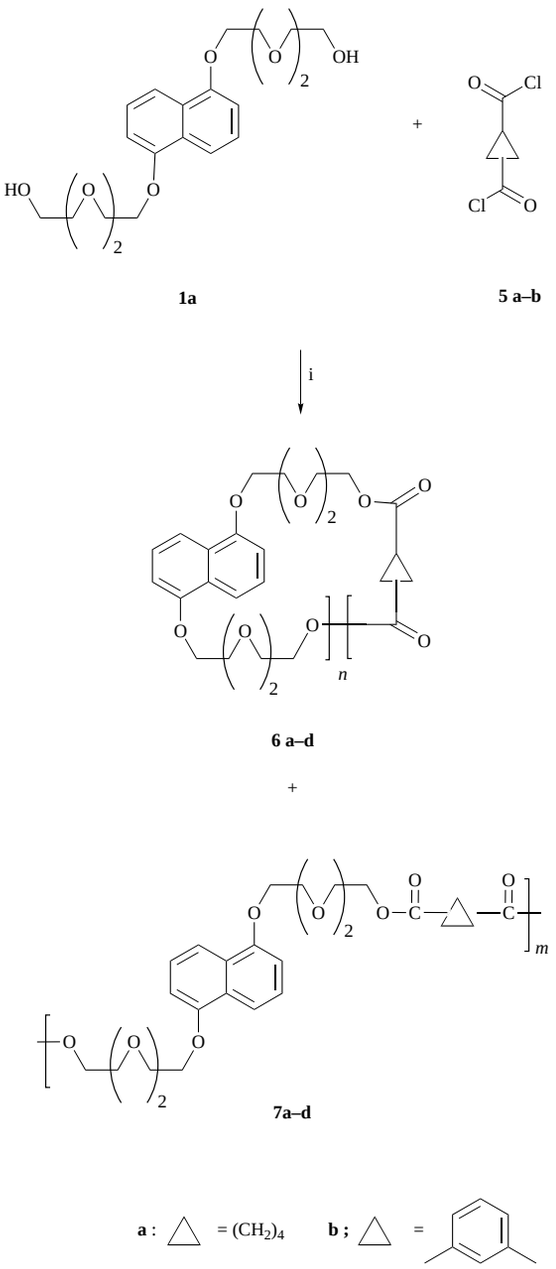


**Scheme 2** *Reagents and conditions*: i, 1,2-dichloroethane, pyridine, reflux

ations between **1a** and **2** as well as **1d** and **2** were performed using various monomer concentrations, both in solution (monomer conc. 0.33 M) and in the melt.[1] The low molecular weight fractions containing **3a**(*n*) and **3d**(*n*), were isolated and analyzed by HPLC using previously isolated **3a**(*n*) and **3d**(*n*) for quantification. The results show that even under concentrated conditions cyclic oligomers are obtained in *ca.* 10 and 2% w/w yield for 0.33 M and melt, respectively (Table 4)! Since generally

**Table 4** Cyclic oligomer yield under concentrated conditions

| Ring[a] | Size[b] | $t_R$(HPLC)/ min | Yield (HPLC) [solution 0.33 M (% w/w)] | Yield (HPLC) [melt (% w/w)] |
|---|---|---|---|---|
| **3a**(1) | 30 | 5.38 | 8.7 | 1.7 |
| **3a**(2) | 60 | 9.81 | 2.3 | 0.3 |
| **3a**(3) | 90 | 11.78 | 0.6 | *c* |
| **3a**(4) | 120 | 12.92 | 0.2 | *c* |
| **3a**(5) | 150 | *c* | *c* | *c* |
| **3d**(1) | 30 | 3.78 | 8.0 | 1.0 |
| **3d**(2) | 60 | 7.18 | 2.4 | 0.9 |
| **3d**(3) | 90 | 9.18 | 1.0 | *c* |

[a] For the physical properties of **3a**(*n*) with $n = 1$–5 and **3d**(*n*) with $n = 1$–3 see Tables 1 and 2, respectively. [b] Size represents the number of atoms determining the ring perimeter. [c] Not observed with HPLC in the crude reaction mixture [for series **3a**(*n*) see also Table 1].

under high dilution conditions cyclic oligomer yields do not exceed 15% w/w yield,[5] these yields are still considerable.

GPC analysis of the high molecular weight fraction after precipitation shows a decrease in molecular weight ($M_r$) for the polymers **4**(**a**–**d**) in going from melt to solution condensation polymerization conditions with decreasing monomer concentrations. For example, molecular weight distributions (GPC) of polymers **4a** and **4d** decrease from $M_r$ $2 \times 10^4$ and $3 \times 10^4$ in the melt, to $M_r$ $1.4 \times 10^4$ and $3.5 \times 10^3$ in solution using monomer concentrations of 0.33 and 0.033 M, respectively.‡ Hence, the weight fraction of cyclic oligomers increases with decreasing concentration of the monomers in the reaction mixture. This is attributed to the different dependence of intramolecular cyclization (first-order kinetics) *versus* intermolecular reactions (second-order kinetics) upon monomer concentrations.[5]

As discussed above, charge-transfer interactions do not appear to play an important role according to cyclic voltammetry and UV–VIS measurements. A more appealing explanation is provided by $^1$H NMR conformational analysis[14] of the 9-hydroxy-1,4,7-trioxanonyl side chains of **1a** and **1d**. As an illustration part of the aliphatic region of the experimental and simulated $^1$H NMR spectrum of the 9-hydroxy-1,4,7-trioxanonyl chain of **1d** ($C_2D_2Cl_4$, 80 °C) is presented in Fig. 3 (see Experimental section). In line with reported data[15] for oligo- and poly-(ethyleneglycols) the HO–[$CH(I)_2$–$CH(II)_2$–O]$_n$– units are present almost exclusively in their *gauche* conformation at 25 and 80 °C. The latter result is of interest since solution condensation polymerization is performed at 80 °C. In Table 5, the *gauche* populations ($x_g$) of the consecutive HO–[$CH(I)_2$–$CH(II)_2$–O]$_n$– units starting at the hydroxy functionality are reported. These results are corroborated by semi-empirical AM1[16] calculations on **1a** and **1d**. For both compounds minima were identified which are close in energy ($\Delta_f H^0$) corresponding to conformers possessing curved 9-hydroxy-1,4,7-trioxanonyl side chains in either an *up-up* or *up-down* relationship (Fig. 4). Whereas for **1a** two minima were found (*up-up* with $C_2$ sym-

‡ In the case of **4b** and **4c** even in the melt $M_r$ does not exceed $5 \times 10^3$. This indicates that condensation polymerization using either **1b** or **1c** as diol mainly gives oligomers (see Experimental section).

**Table 5** $^1$H NMR conformational analysis of the HO–[CH(I)$_2$–CH(II)$_2$–O]$_n$– units of the 9-hydroxy-1,4,7-trioxanonyl side chains of **1a** and **1d**[a]

| | *n* | | | | | |
|---|---|---|---|---|---|---|
| | **1a** | | | **1d** | | |
| | 1 | 2 | 3 | 1 | 2 | 3 |
| $x_g$ (25 °C, $CD_2Cl_2$) | 0.94 | 0.92 | 0.91 | 0.94 | 0.94 | 0.92 |
| $x_g$ (80 °C, $C_2D_2Cl_4$) | 0.92 | 0.88 | 0.85 | 0.91 | 0.88 | 0.85 |

[a] $n$ = 1, 2 and 3 represent the HO–[CH(I)$_2$–CH(II)$_2$–O]$_n$– units starting from the hydroxy functionality; $x_g$ *gauche* population with $x_g + x_a = 1$. With both $J_{ab/ax}$ and $J_{ab'/ax'}$ consistent results were obtained (*cf.* ref. 15 and see Experimental section).

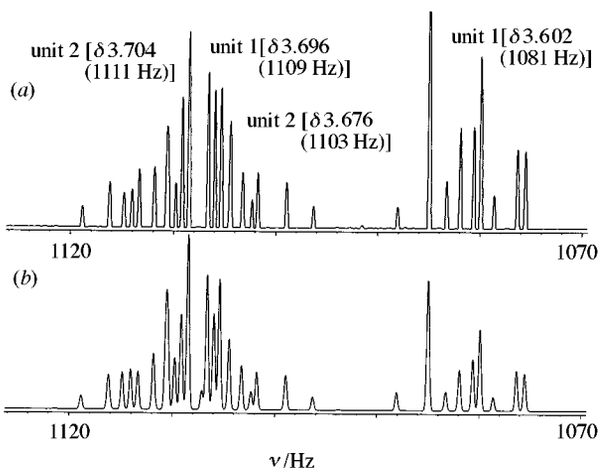


**Fig. 3** $^1$H NMR spectrum of **1d**; comparison of the Ar–OCH$_2$–CH$_2$–OC*H*(II)$_2$C*H*(I)$_2$–OC*H*(II)$_2$C*H*(I)$_2$OH, *viz*. units 1 and 2 [upper trace, experimental (solvent $C_2D_2Cl_4$, 80 °C) and lower trace, simulated; see also Tables 5 and 8]

metry and *up-down* with $C_i$ symmetry), for **1d** four minima were identified (*up-up* with either $C_2$ or $C_s$ symmetry and *up-down* with either $C_2$ or $C_i$ symmetry). The calculations unequivocally show that the HO–[CH(I)$_2$–CH(II)$_2$–O]$_n$– units possess a *gauche* conformation, while the torsion angles across the C–O bonds are close to antiperiplanar (Table 6). Note that our gas phase calculations predict substantial dipole moments for the *up-up* isomers of **1a** ($C_2$ symmetry, $\mu$ 2.87 D) and **1d** ($C_2$ symmetry, $\mu$ 2.51 D and $C_s$ symmetry, $\mu$ 3.14 D). In contrast, the dipole moments $\mu$ of the *up-down* isomers of **1a** and **1d** possessing $C_i$ symmetry are zero, while **1d** with $C_2$ symmetry has a reduced dipole moment ($\mu$ 1.78 D). Hence, to a first approximation the *up-up* isomers of **1a** and **1d** will be (more) stabilized in a solvent, such as that used in our solution polycondensation reactions (1,2-dichloroethane; $\varepsilon$ 10.42[17]) due to favourable solute–solvent interactions.§[18] Furthermore, taking into account the low rotational barrier across an aryl C–O bond,[19] we conclude that as a consequence of the preferred *gauche* conformation of the HO–[CH(I)$_2$–CH(II)$_2$–O]$_n$– units the 9-hydroxy-1,4,7-trioxanonyl side chains of the diols **1a**–**d** possess a curved geometry leading to favourable pre-orientation for intramolecular cyclization during condensation polymerization.

§ To a first-order approximation the stabilization energy due to solute–solvent interactions upon dissolution of a polar compound can be described by $E = -1/2f\mu^2$ in which $\mu$ [1 D (Debye) = 3.33564 × 10$^{-30}$ C m] is the dipole moment of the solute and $f = 2/V(\varepsilon - 1/2\varepsilon + 1)$ with $V$ being the effective volume of the cavity occupied by the solute in the particular solvent and $\varepsilon$ the relative permittivity of the solvent.[18] It is assumed that the *up-up* and *up-down* isomers of **1a** and **1d**, respectively, possess an identical effective volume $V$.

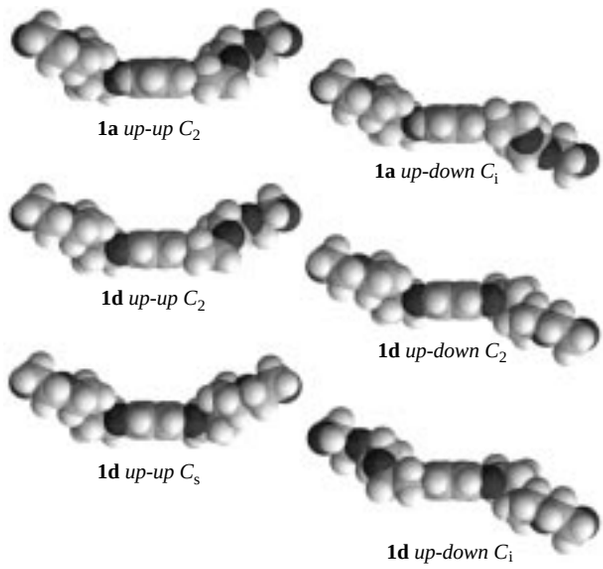


**Fig. 4** AM1[16] optimized structures of conformers of **1a** and **1d**, respectively, with the 9-hydroxy-1,4,7-trioxanonyl side chains either *up-up* or *up-down*. AM1 O–CH$_2$–CH$_2$–O torsion angles are reported in Table 6.

### Single crystal X-ray structure determination of 3a(1), 3d(1) and 6a(1)

In recent years a variety of single crystal X-ray structures of both symmetrical and asymmetrical crownophanes have been reported.[9,10,20] The cyclic oligomers **3a**(*n*), **3d**(*n*) and **6a**(*n*) are representatives of the latter class. Suitable crystals for single crystal X-ray structure determination of **3a**(1) and **3d**(1) were obtained *via* vapour diffusion crystallization (solvent dichloromethane/non-solvent *n*-hexane). In the case of **6a**(1) slow evaporation of a column chromatography (eluent: acetone–*n*-hexane 1:1 v/v) fraction afforded appropriate crystals (see Experimental section). Unfortunately, suitable crystals for single crystal X-ray structure determination of the higher homologues with, for example, $n = 2$ have hitherto not been obtained. Further work is in progress.

In Fig. 5, ORTEP representations (50% probability level) of **3a**(1), **3d**(1) and **6a**(1) are shown. In the case of **3a**(1), one of the 1,4,7-trioxanonyl bridges possesses conformational disorder [ratio 0.849(9): 0.151(9)] for atoms O(25), H(241), H(242), H(261) and H(262). With the exception of the torsion angle O(25)–C(26)–C(27)–O(28) of 164.1(3)° (close to antiperiplanar), all –O–[CH(I)$_2$–CH(II)$_2$–O]$_n$– units in **3a**(1) possess a nearly *gauche* conformation with torsion angles in the range 66.7–81.1°. Bond lengths, valence angles and torsion angles are in line with expectation. Inspection of the packing motif of **3a**(1) reveals that its cavity is occupied by both a terephthaloyl and a bis-substituted naphthalene unit of two symmetry related molecules. In the solid state **3a**(1) is self-complementary; it possesses both host and guest behaviour. This is attributed to the presence of weak non-covalent edge–face arene–arene contacts[21] between both terephthaloyl–naphthalene and naphthalene–naphthalene moieties; the centres of gravity (CG) of the six-membered rings of the naphthyl [CG(1) and CG(2)] and terephthaloyl [CG(3)] units of symmetry related molecules **3a**(1) [distance *d*(CG–CG) range 4.792–5.482 Å] and their interplanar torsion angles (range 46–88°) are in line with those expected for attractive edge–face arene–arene interactions.[21] The packing motif is complemented by minimalization of unfavourable dipole–dipole interactions between neighbouring terephthaloyl units which possess a (partial) dipole moment (AM1;[16] model compound, dimethyl terephthalate $\mu$ 2.79 D), *i.e.* the inversion symmetry related terephthaloyl units of molecules **3a**(1) pack face-to-face. Furthermore, weak inter- and

**Table 6** AM1 O–$CH_2$–$CH_2$–O torsion angles of the HO–[$CH(I)_2$–$CH(II)_2$–O]$_n$– units $n$ = 1, 2 and 3 of the 9-hydroxy-1,4,7-trioxanonyl side chains of **1a** and **1d**

| | H–[O–$CH(I)_2$–$CH(II)_2$–O]$_n$–/° | | | |
|---|---|---|---|---|
| Compound (unit[a]) | *up-up* $C_2$ sym. | *up-up* $C_s$ sym. | *up-down* $C_2$ sym. | *up-down* $C_i$ sym. |
| **1a**(1) | 67.4 | — | — | 67.4 |
| **1a**(2) | −95.1 | — | — | −95.7 |
| **1a**(3) | 92.0 | — | — | 91.7 |
| $\Delta_f H^0$/kcal mol$^{-1}$[b] | −327.3 | — | — | −327.3 |
| $\mu$/D[c] | 2.87 | — | — | 0.00 |
| **1d**(1) | 67.4 | 67.4 | 67.4 | 67.4 |
| **1d**(2) | −96.0 | −96.3 | −96.6 | −96.6 |
| **1d**(3) | 93.6 | 93.6 | 93.4 | 93.4 |
| $\Delta_f H^0$/kcal mol$^{-1}$[b] | −347.1 | −347.2 | −347.2 | −347.1 |
| $\mu$/D[c] | 2.51 | 3.14 | 1.78 | 0.00 |

[a] $n$ = 1, 2 and 3 represent the HO–[$CH(I)_2$–$CH(II)_2$–O]$_n$– units starting from the hydroxy functionality (see Table 5). [b] 1 cal = 4.184 J. [c] 1 D (Debye) = $3.33564 \times 10^{-30}$ Cm.

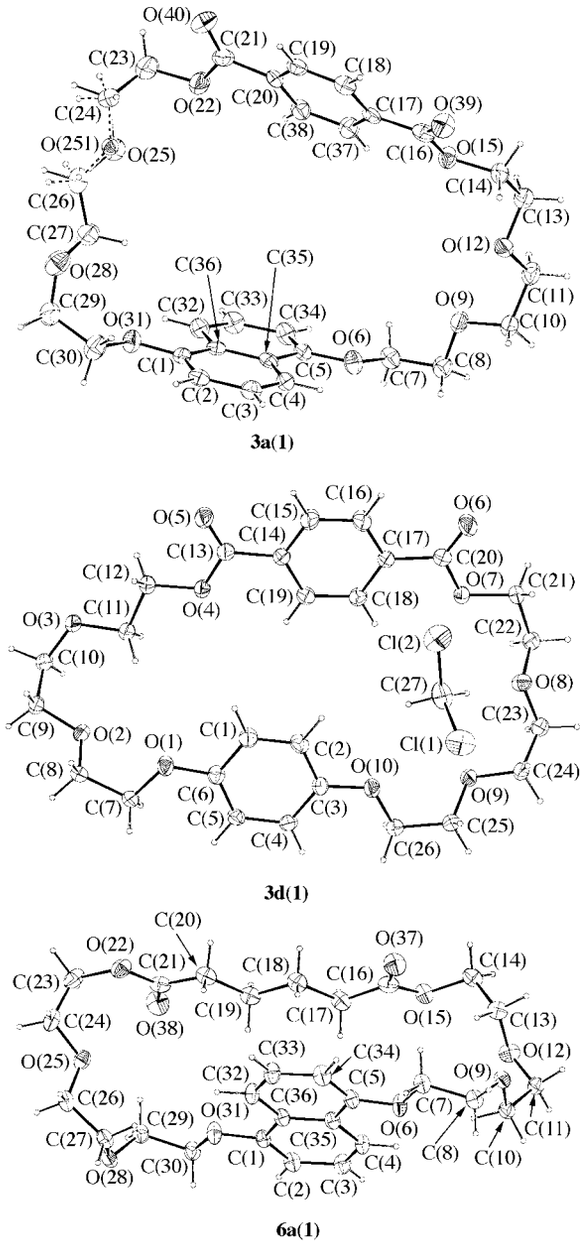


**Fig. 5** ORTEP plots (50% probability) of the crownophanes **3a**(1), **3d**(1) and **6a**(1). Atom numberings of **3a**(1), **3d**(1) and **6a**(1) are not in agreement with IUPAC guidelines (see Experimental section).

intra-molecular C–H···O interactions are found (Table 7). This leads to a packing motif which consists of infinite sheets of interpenetrating molecules **3a**(1) in the *bc* plane at $a$ = 1/2,

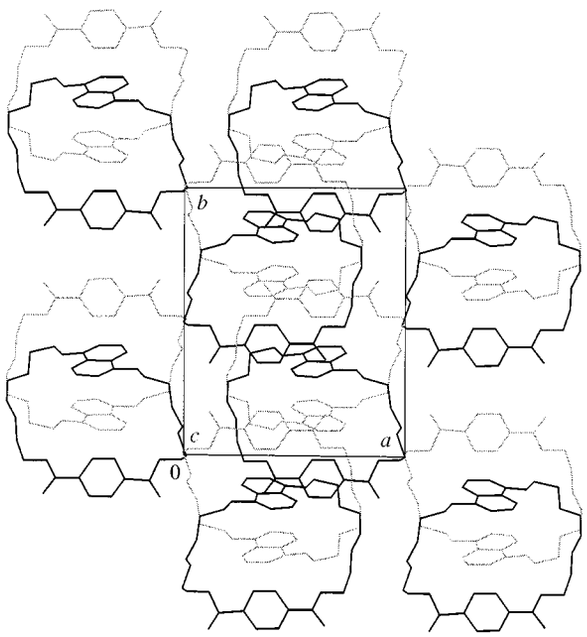


**Fig. 6** Packing motif of **3a**(1); projection in the *ab*-plane (hydrogen atoms are omitted for clarity).[10] The highlighted molecules **3a**(1) occupy the cavity of a symmetry-related molecule **3a**(1) depicted shaded.

which are separated at $a$ = 0 and $a$ = 1 by oligo(ethyleneglycol) chain layers (Fig. 6). An estimate of the packing ratio, *i.e.* the percentage of the unit cell volume actually occupied by atoms in the solid state, was obtained by combining the single crystal unit cell volume, the number of crystallographically independent molecules and the molecular volume determined with a calculational procedure such as MOLSV.¶[22] Despite its 30 atom perimeter, in the solid state **3a**(1) packs efficiently, a packing ratio of 71.8% is found.[10]

In the case of **3d**(1) the bond lengths, valence angles and torsion angles are also in line with expectation. With the exception of the O(3)–C(11)–C(12)–O(4) bond angle of 177.09(13)° (close to antiperiplanar), all –O–[$CH(I)_2$–$CH(II)_2$–O]$_n$– units in **3d**(1) possess a nearly *gauche* conformation with torsion angles in the range 64.6–76.4°. However, exchange of the bis-substituted naphthalene core by a phenyl core leads to considerable changes in the solid-state packing motif. In contrast to **3a**(1) attractive edge–face arene–arene interactions are absent (Fig. 7). Moreover, a characteristic feature of the single crystal X-ray structure of **3d**(1) is the presence of one molecule of

¶ In the MOLSV[22] calculations the single crystal X-ray structures were used as input data.

**Table 7** Solid state inter- and intra-molecular C–H · · · O interactions for **3a**(1), **3d**(1) and **6a**(1)[a]

| Compound | C(a)–H(b) · · · O(c) | Type | *d*(C · · · O)/Å | *d*(H · · · O)/Å | Angle C–H · · · O/° |
|---|---|---|---|---|---|
| **3a**(1) | C(23)–H(231) · · · O(40) | intra | 2.675 | 2.320 | 100.7 |
| | C(27)–H(271) · · · O(40) | inter | 3.461 | 2.568 | 152.8 |
| | C(3)–H(31) · · · O(9) | inter | 3.281 | 2.505 | 141.0 |
| | C(11)–H(11) · · · O(28) | inter | 3.461 | 2.515 | 164.9 |
| **3d**(1) | C(11)–H(11B) · · · O(2) | intra | 3.014 | 2.420 | 117.9 |
| | C(1)–H(1) · · · O(1) | inter | 3.493 | 2.562 | 166.5 |
| | C(5)–H(5) · · · O(6) | inter | 3.423 | 2.482 | 170.6 |
| | C(10)–H(10B) · · · O(9) | inter | 3.459 | 2.512 | 159.9 |
| **6a**(1) | C(10)–H(101) · · · O(6) | intra | 3.121 | 2.475 | 121.3 |
| | C(13)–H(132) · · · O(9) | intra | 3.006 | 2.437 | 118.1 |
| | C(23)–H(231) · · · O(38) | intra | 2.683 | 2.275 | 103.7 |
| | C(27)–H(271) · · · O(31) | intra | 3.162 | 2.517 | 127.3 |
| | C(29)–H(291) · · · O(25) | intra | 3.099 | 2.412 | 126.9 |
| | C(14)–H(142) · · · O(22) | inter | 3.450 | 2.595 | 142.1 |
| | C(14)–H(141) · · · O(28) | inter | 3.405 | 2.522 | 145.7 |
| | C(34)–H(341) · · · O(38) | inter | 3.116 | 2.40 | 128.4 |

[a] Atom numberings of **3a**(1), **3d**(1) and **6a**(1) are not in agreement with IUPAC guidelines (see Experimental section).



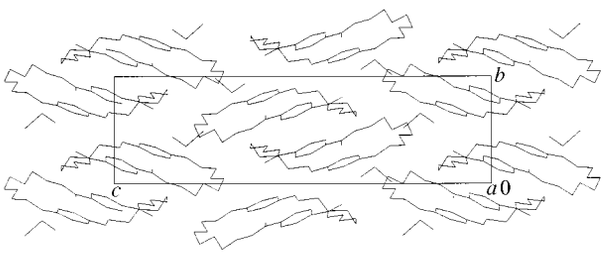


**Fig. 7** Packing motif of **3d**(1) with the complexed dichloromethane moiety; view along the *a*-axis. Hydrogen atoms are omitted for clarity.

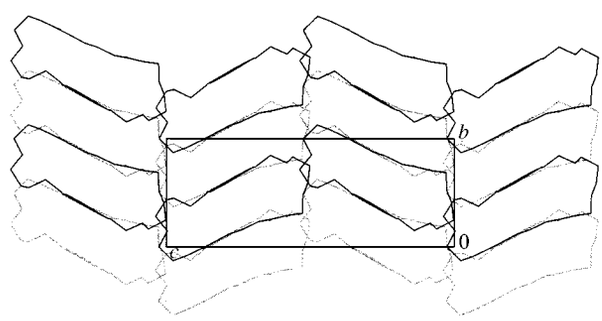


**Fig. 8** Packing motif of **6a**(1); view along the *a*-axis. Hydrogen atoms are omitted for clarity. The second layer of molecules **6a**(1), which is shifted 1/2*a*, 1/2*b*, 0, is highlighted.

dichloromethane per cyclic oligomer. It is well documented that crown ethers containing neutral guest molecules can be stabilized by either favourable dipole–dipole or hydrogen-bonding interactions.[23] A C–H · · · O interaction [C(27)–H(27B) · · · O(8), C · · · O 3.220(3) Å, H · · · O 2.231(3) Å, C–H · · · O 176.7(2)°] is observed between the dichloromethane moiety and the macrocycle together with short dipole–dipole contacts {[Cl(1)–H(23B) 2.841(2) Å] and [Cl(2)–C(20) 3.333(2) Å], Fig. 5}; additional C–H · · · O interactions are listed in Table 7. For **3d**(1) a packing ratio of 68.3% (MOLSV[22]) was determined, also taking into account the presence of the complexed dichloromethane.

Since for **6a**(1) the incorporated bis-acid chloride **5a** is aliphatic, edge–face interactions between the diol and bis-acid moiety will be impaired. Again the bond lengths, valence angles and torsion angles are within expectation. All –O–[$CH(I)_2$–$CH(II)_2$–O]$_n$– units possess a *gauche* conformation with torsion angles in the range 61.1–80.5°. Molecules **6a**(1) pack in stacks parallel to the *b*-axis with the plane of the bis-substituted naphthalene moieties oriented perpendicular to the *b*-axis. The stacks display a herringbone structure tilted with respect to the *b*-axis (Fig. 8). A packing ratio of 70.4% (MOLSV[22]) is found. Both inter- and intra-molecular CH · · · O interactions discernible in its solid-state packing motif are listed in Table 7.

## Conclusions

Condensation polymerization of bis(9-hydroxy-1,4,7-trioxanonyl) substituted aromatics (**1a**–**d**) with bis-acid chlorides **2**, **5a** and **5b**, both in the melt as well as in solution using two different monomer concentrations (0.33 and 0.033 M) gives access to considerable amounts of cyclic oligomers, *i.e.* crownophanes [melt, 2% w/w and solution (0.033 M) 30% w/w and (0.33 M) 10% w/w]. Crownophanes with atom perimeters up to 150 atoms were isolated. $^1$H NMR conformational analysis of the 9-hydroxy-1,4,7-trioxanonyl side chains at 25 and 80 °C, *viz*. the temperature used for solution condensation polymerization, reveals that all H–[O–$CH(I)_2$–$CH(II)_2$–O]$_n$– units are mainly present in their *gauche* conformation. These experimental data are supported by semi-empirical AM1 calculations and indicate that the side chains possess a curved geometry. Hence, they will be pre-oriented for intramolecular ring closure. The results show that cyclic oligomer yields are not influenced by the type of bis-acid chloride used. Single crystal X-ray structure determinations of **3a**(1), **3d**(1) and **6a**(1) show that the solid-state packing motifs of these floppy cyclic oligomers are affected by the type of diol and bis-acid constituents.

## Experimental

### General

All syntheses were carried out under a dry nitrogen atmosphere unless stated otherwise. Solvents were dried using standard procedures. NMR spectra were recorded on a Bruker AC300 operating at 300 ($^1$H NMR) and 75 MHz ($^{13}$C NMR). Chemical shifts are given relative to external TMS and all coupling constants *J* are in Hz. All NMR measurements were performed in $CDCl_3$ unless stated otherwise. FTIR spectra were recorded on a Mattson Galaxy Series FTIR 5000 Spectrometer using a diffuse reflection accessory; samples were diluted in KBr. Dispersive IR spectra (NaCl plates or KBr pellets) were recorded on a Perkin-Elmer 283 spectrophotometer. UV–VIS spectroscopy was carried out on a Cary 1 in spectrophotometric grade acetonitrile. HPLC was performed on a reversed phase $C_{18}$ column (either 3 or 5 μ particles, column diameter 4.6 mm and length 10 cm) using gradient elution [acetonitrile : water 1 : 1 (v/v) to 1 : 0 (v/v); elution velocity 1 ml min$^{-1}$] and UV–detection (λ 254 nm). Gel permeation chromatography (GPC) was performed using a mixed bed column with THF as eluent and both UV (λ 254 nm) and RI detection. Differential scanning calorimetry (DSC, Mettler DSC 12E) was carried out at a heating rate of 5 °C min$^{-1}$ and cooling rates of 1–5 °C min$^{-1}$. Melt enthalpies

**Table 8** Coupling constants $J_{ab/ax}$ and $J_{ab'/ax'}$ for the AA′BB′ and AA′XX′ patterns of the HO–[C$H(I)_2$–C$H(II)_2$–O]$_n$– units of the 9-hydroxy-1,4,7-trioxanonyl side chains of **1a** and **1d** taken from simulated $^1$H NMR spectra at 25 ($CD_2Cl_2$) and 80 °C ($C_2D_2Cl_4$) (see also Table 5)

| Compound (unit) | $J_{ab/ax}$/Hz | | $J_{ab'/ax}$/Hz | | $J_{aa'}$/Hz | | $J_{bb'}$/Hz | |
|---|---|---|---|---|---|---|---|---|
| | 25 °C | 80 °C | 25 °C | 80 °C | 25 °C | 80 °C | 25 °C | 80 °C |
| **1a**(1)[a] | 2.97 | 3.15 | 6.29 | 6.24 | −10.41 | −10.38 | −12.01 | −11.66 |
| **1a**(2)[a] | 3.10 | 3.52 | 6.24 | 6.14 | −10.41 | −11.47 | −11.04 | −11.47 |
| **1a**(3)[a] | 3.27 | 3.75 | 6.17 | 6.18 | −10.63 | −10.22 | −11.13 | −10.85 |
| **1d**(1)[b] | 2.91 | 3.21 | 6.30 | 6.24 | −10.43 | −10.57 | −12.05 | −11.92 |
| **1d**(2)[b] | 2.94 | 3.50 | 6.31 | 6.19 | −10.94 | −10.81 | −11.01 | −10.81 |
| **1d**(3)[b] | 3.17 | 3.83 | 6.21 | 6.12 | −10.59 | −10.65 | −11.07 | −11.19 |

[a] Chemical shifts of **1a** for the HO–[C$H(I)_2$–C$H(II)_2$–O]$_n$– units $n$ = 1, 2 and 3, at 25 °C [unit 1 $\delta(I)$ 3.574 and $\delta(II)$ 3.659, unit 2 $\delta(I)$ 3.682 and $\delta(II)$ 3.768 and unit 3 $\delta(I)$ 3.972 and $\delta(II)$ 4.290] and at 80 °C [unit 1 $\delta(I)$ 3.614 and $\delta(II)$ 3.694, unit 2 $\delta(I)$ 3.709 and $\delta(II)$ 3.788 and unit 3 $\delta(I)$ 3.984 and $\delta(II)$ 4.325]. [b] Chemicals shifts of **1d** for the HO–[C$H(I)_2$–C$H(II)_2$–O]$_n$– units $n$ = 1, 2 and 3, at 25 °C [unit 1 $\delta(I)$ 3.562 and $\delta(II)$ 3.657, unit 2 $\delta(I)$ 3.648 and $\delta(II)$ 3.677 and unit 3 $\delta(I)$ 3.791 and $\delta(II)$ 4.060] and at 80 °C [unit 1 $\delta(I)$ 3.602 and $\delta(II)$ 3.696, unit 2 $\delta(I)$ 3.676 and $\delta(II)$ 3.704 and unit 3 $\delta(I)$ 3.812 and $\delta(II)$ 4.090].

($\Delta H$) are reported in cal g$^{-1}$. Cyclic voltammograms were recorded with a Heka Potentiostat (Type: PG287; 220 V/50 Hz) using a platinum electrode and a scan rate of 100 mV s$^{-1}$ in dry acetonitrile with tetrabutylammonium hexafluorophosphate (TBAP) as electrolyte (0.1 M) and an Ag/$AgNO_3$ reference electrode. To reference all electrochemical data to SCE values the ferrocene/ferrocenium couple was used. FABMS spectra were measured on a JEOL JMS SX/SX 102A four-sector mass spectrometer operated at either 10 kV (resolution 2400 amu) or 8 kV (resolution 3100 amu) with a JEOL MSFAB 10D FAB gun operated with a 10 mA emission current (matrix *m*-nitrobenzyl alcohol). Elemental analyses were carried out by H. Kolbe Mikroanalytisches Laboratorium, Mülheim a.d. Ruhr, Germany.

### $^1$H NMR conformational analysis

$^1$H NMR measurements on compounds **1a** (15 mg) and **1d** (15 mg) were performed on filtered solutions in $CD_2Cl_2$ (0.5 ml) and $C_2D_2Cl_4$ (0.5 ml) at 25 and 80 °C, respectively. $D_2O$ (20 µl) was added to suppress coupling of the hydroxy proton with its neighbouring $CH_2$ group. At least 256 scans were accumulated with a file size of 32 kbyte. After zero filling to 128 kbyte a Gaussian enhancement (25 °C: **1a**, LB −5.0 and GB 0.3 and **1d**, LB −1.0 and GB 0.3. 80 °C: **1a**, LB −2.0 and GB 0.5 and **1d**, LB −2.0 and GB 0.5 using the WIN-NMR program[14]) was applied; a resolution of 0.07 Hz per point was obtained. The chemical shifts $\delta$ and coupling constants $J_{ab/ax}$ and $J_{ab'/ax'}$ for the AA′BB′/AA′XX′ systems of the HO–[CH(I)$_2$–CH(II)$_2$–O]$_n$– sequences in both **1a** and **1d** at 25 and 80 °C were derived from simulated $^1$H NMR spectra using the GeNMR (version 3.5.1)[14] computer program (Table 8). The *anti* ($x_a$) and *gauche* ($x_g$) populations were calculated from the experimental coupling constants using eqn. (1) taken from ref. 15, where for

$$x_g = \frac{2(J_t^t - J_{ab/ax})}{2J_t^t - J_g^{gx} - J_g^{gy}} = \frac{2(J_t^g - J_{ab'/ax'})}{2J_t^g - J_g^{g'} - J_g^t} \qquad (1)$$

X–$CH_2$–$CH_2$–Y with X = Y = O $J_t^t$ 11.91, $J_t^g$ 5.80, $J_g^t$ 12.27, $J_g^{gx} = J_g^{gy}$ 2.36 and $J_g^{g'}$ 0.44 Hz. In eqn. (1) *t* represents *trans*, *vis*. *anti* and *g* represents *gauche*. For an explanation of $J_t^t$, $J_t^g$, $J_g^t$, $J_g^{gx}$, $J_g^{gy}$ and $J_g^{g'}$ we refer to the original reference.[15] Both $J_{ab/ax}$ and $J_{ab'/ax'}$ gave consistent results (see Table 5). For chemical shifts see Table 8.

### Semi-empirical AM1 calculations

Calculations were performed with AM1[16] as implemented in MOPAC 7.0.[16] Preoptimized MMX[16] geometries were further optimized without symmetry constraints until GNORM ≤ 0.01 using the eigenvector following (EF) routine of MOPAC 7.0. Minima were characterized by a Hessian calculation (keywords FORCE and LARGE); no imaginary vibrations were found. Heats of formation ($\Delta_f H^0$) are reported in kcal mol$^{-1}$ (1 cal = 4.184 J). Data concerning the geometry optimization, optimized geometries and the Hessian calculations are available upon request from one of the authors (L. W. J.).

### Single crystal X-ray structures of 3a(1), 3d(1) and 6a(1)

Suitable crystals for single crystal X-ray structure determination of **3a**(1)[10] and **3d**(1) were obtained *via* vapour diffusion crystallization (solvent dichloromethane/non-solvent *n*-hexane). In the case of **6a**(1) slow evaporation of a column chromatography (eluent: acetone–*n*-hexane 1:1 v/v) fraction afforded appropriate crystals.

**Crystal data for 3a(1).**[10] $C_{30}H_{34}O_{10}$, $M$ = 554.59, colourless plate shaped crystal (0.05 × 0.30 × 0.62 mm), monoclinic, $P2_1/c$, $a$ = 13.8318(11) Å, $b$ = 16.0285(9) Å, $c$ = 12.5574(11) Å, $\beta$ = 107.56(1)°, $V$ = 2654.3(4) Å$^3$, $Z$ = 4, $d_{calc}$ = 1.388 g cm$^{-3}$, $F(000)$ = 1176, $\mu$(Mo-Kα) = 1.0 cm$^{-1}$, 7889 reflections (1.27 < $\theta$ < 24.18°, $\omega/2\theta$ scan; $T$ = 150 K) were measured on an Enraf–Nonius CAD-4T diffractometer [rotating anode, graphite monochromated Mo-Kα radiation ($\lambda$ = 0.710 73 Å)]. Data were corrected for Lorentzian and polarization (Lp) effects and for a linear decay (1%) of the intensity control reflections and merged into a data set of 3928 unique reflections ($R_i$ = 0.0540). The structure was solved by direct methods (SHELXS-86)[24] and difference Fourier techniques. One of the oxygen atoms [O(25)] within the ring is disordered [0.151(9):0.849(9)] over two positions. Hydrogen atoms were introduced at calculated positions and refined riding on their carrier atoms. All non-H atoms (except the minor disordered O atom) were refined on $F^2$ (SHELXL-93)[25] using all 3928 unique reflections, with anisotropic thermal parameters. Convergence was reached at $R_1$ = 0.0548 for 2198 reflections with $I > 2.0\sigma(I)$ and 367 parameters; $wR_2$ = 0.1189, $S$ = 0.95 for all 3928 reflections, $w = 1/[\sigma^2(F) + (0.0473P)^2]$. A final difference Fourier map shows no residual density outside −0.35:0.39 e Å$^{-3}$.

**Crystal data for 3d(1).** $C_{26}H_{32}O_{10}\cdot CH_2Cl_2$, $M_r$ = 589.46, colourless block shaped crystal (0.50 × 0.50 × 0.50 mm), monoclinic, space group $P2_1/c$, with $a$ = 13.1880(13) Å, $b$ = 7.9223(5) Å, $c$ = 27.379(2) Å, $\beta$ = 92.19(1)°, $V$ = 2858.4(4) Å$^3$, $Z$ = 4, $d_{calc}$ = 1.370 g cm$^{-3}$, $F(000)$ = 1240, $\mu$(Mo-Kα) = 2.8 cm$^{-1}$; 7311 reflections (0.75 < $\theta$ < 27.50°; $\omega/2\theta$ scan; $T$ = 150 K) were measured on an Enraf–Nonius CAD-4T diffractometer [rotating anode, graphite monochromated Mo-Kα radiation ($\lambda$ = 0.710 73 Å)]. Data were corrected for a linear decay (1.2%) of the intensity control reflections and merged into a dataset of 6502 unique reflections. The structure was solved with direct methods (SHELXS-86)[24] and difference Fourier techniques. Hydrogen atoms were introduced at calculated positions and refined riding on their carrier atoms. All non-H atoms were refined on $F^2$ (SHELXL-93)[25] using 6486 unique reflections, with anisotropic thermal parameters. Convergence was reached at $R_1$ = 0.0443 for 4813 reflections with $F_o > 4.0\sigma(F_o)$ and 352 parameters; $wR_2$ = 0.1124, $S$ = 1.044 for 6486 reflections, $w = 1/[\sigma^2(F_o^2) + (0.0553\ P)^2 + 0.73\ P]$. A final

difference Fourier map shows no residual density outside −0.38 : 0.34 e Å$^{-3}$.

**Crystal data for 6a(1).** $C_{28}H_{38}O_{10}$, $M_r$ = 534.60, colourless block shaped crystal (0.45 × 0.50 × 0.50 mm), monoclinic, space group $C_c$, with $a$ = 14.8295(6) Å, $b$ = 8.2246(5) Å, $c$ = 21.8040(15) Å, $\beta$ = 92.44(1)°, $V$ = 2656.9(3) Å$^3$, $Z$ = 4, $d_{calc}$ = 1.337 g cm$^{-3}$, $F(000)$ = 1144, $\mu$(Mo-Kα) = 1.0 cm$^{-1}$; 3644 reflections (0.94 < $\theta$ < 27.45°; $\omega$ scan; $T$ = 150 K) were measured on an Enraf–Nonius CAD-4T diffractometer [rotating anode, graphite monochromated Mo-Kα radiation ($\lambda$ = 0.710 73 Å)]. Data were corrected for a linear decay (1.3%) of the intensity control reflections and merged into a dataset of 3399 unique reflections. The structure was solved with direct methods (SHELXS-86)[24] and difference Fourier techniques. Hydrogen atoms were introduced at calculated positions and refined riding on their carrier atoms. All non-H atoms were refined on $F^2$ (SHELXL-93)[25] using the 3399 unique reflections, with anisotropic thermal parameters. Convergence was reached at $R_1$ = 0.0404 for 3091 reflections with $F_o > 4.0\sigma(F_o)$ and 365 parameters; $wR_2$ = 0.1048, $S$ = 1.056 for 3399 reflections, $w = 1/[\sigma^2(F_o^2) + (0.0743\ P)^2 + 0.176\ P]$. A final difference Fourier map shows no residual density outside −0.29 : 0.22 e Å$^{-3}$.

Full crystallographic details of **3a**(1),[10] **3d**(1) and **6a**(1), excluding structure factor tables, have been deposited at the Cambridge Crystallographic Data Centre (CCDC). For details of the deposition scheme, see 'Instructions for Authors', *J. Chem. Soc.*, *Perkin Trans. 2*, available *via* the RSC Web pages (http://www.rsc.org/authors). Any request to the CCDC for this material should quote the full literature citation and the reference number 188/112.

## Syntheses

All bis(9-hydroxy-1,4,7-trioxanonyl) substituted aromatics were synthesized using modified literature procedures.[26–28]

**1,5-Bis(9-hydroxy-1,4,7-trioxanonyl)naphthalene (1a).** To a solution of 1,5-dihydroxynaphthalene (22.0 g, 0.136 mol) and 2-[2-(2-chloroethoxy)ethoxy]ethanol (48.0 g, 0.284 mol) in DMF (500 ml) potassium carbonate (57 g, 0.41 mol) was added under vigorous stirring. After stirring the suspension at 50 °C for 3 days, the solvent was removed under reduced pressure. The dark viscous residue was triturated with methylene chloride after which the precipitated salts were removed by filtration. The filtrate was concentrated under reduced pressure to yield crude **1a**, which was recrystallized twice from acetone (1 g/20 ml) to yield 34 g (80.2 mmol, 59%) of an off-white powder. Mp 68–69 °C (lit.,[26] 67–68 °C); $\delta_H$ 7.87 (d, 2H, $J$ 8.4), 7.35 (dd, 2H, $J$ 8.4, 7.6), 6.84 (d, 2H, $J$ 7.6), 4.32–4.28 (m, 4H), 4.01–3.98 (m, 4H), 3.82–3.79 (m, 4H), 3.73–3.70 (m, 8H), 3.62–3.60 (m, 4H) and 2.45 (br s, 2H) (see also Table 5); $\delta_C$ 154.3, 126.8, 125.1, 114.6, 105.7, 72.5, 71.0, 70.5, 69.8, 67.9 and 61.8; $\nu_{max}$(FTIR, KBr)/cm$^{-1}$ 3430 (broad), 1271, 1122, 1081.

**1,2-Bis(9-hydroxy-1,4,7-trioxanonyl)benzene (1b).** Catechol (11.0 g, 0.100 mol), 2-[2-(2-chloroethoxy)ethoxy]ethanol (34.0 g, 0.202 mol), potassium carbonate (42 g, 0.3 mol) and DMF (250 ml) were used (*cf*. compound **1a** for procedures). Workup after 3 days gave a brown oil as the crude product. After flash chromatography on silica gel [230–400 mesh, eluent ethyl acetate (750 ml)] to remove impurities compound **1b** was eluted from the column with methanol. Removal of the solvent under reduced pressure gave 12.8 g (34.2 mmol, 34%) of **1b** as a light yellow oil. $\delta_H$ 6.87 (s, 4H), 4.15–4.11 (m, 4H), 3.84–3.80 (m, 4H), 3.71–3.63 (m, 12H), 3.61–3.56 (m, 4H) and 3.34 (br s, 2H); $\delta_C$ 148.6, 121.5, 114.6, 72.4, 70.5, 70.1, 69.5, 68.6 and 61.3; $\nu_{max}$(IR, NaCl)/cm$^{-1}$ 3330 (broad), 1255, 1112, 1065.

**1,3-Bis(9-hydroxy-1,4,7-trioxanonyl)benzene (1c).** Resorcinol (11.0 g, 0.100 mol), 2-[2-(2-chloroethoxy)ethoxy]ethanol (34.0 g, 0.202 mol), potassium carbonate (42 g, 0.30 mol) and DMF (250 ml) were used (*cf*. compound **1a** for procedures). Workup after 8 days gave the crude product as a dark red oil. Impurities were removed by flash chromatography on silica gel [230–400 mesh, eluent ethyl acetate (750 ml)], after which compound **1c** was eluted from the column with methanol. Removal of the solvent under reduced pressure gave 29.4 g (78.5 mmol, 78%) of **1c** as a colourless oil. $\delta_H$ 7.12 (m, 1H), 6.50–6.47 (m, 3H), 4.10–4.07 (m, 4H), 3.83–3.80 (m, 4H), 3.71–3.64 (m, 12H), 3.59–3.56 (m, 4H) and 2.74 (t, 2H, $J$ 5.9); $\delta_C$ 159.8, 129.7, 107.1, 101.8, 72.4, 70.7, 70.3, 69.6, 67.3 and 61.6; $\nu_{max}$(IR, NaCl)/cm$^{-1}$ 3460 (broad), 1120, 1065.

**1,4-Bis(9-hydroxy-1,4,7-trioxanonyl)benzene (1d).** Hydroquinone (11.0 g, 0.100 mol), 2-[2-(2-chloroethoxy)ethoxy]ethanol (34.0 g, 0.202 mol), potassium carbonate (42 g, 0.30 mol) and DMF (250 ml) were used (*cf*. compound **1a** for procedures). Workup after 5 days gave a pink solid which was recrystallized from acetone (1 g/20 ml) to yield 17.9 g (47.8 mmol, 48%) of a white solid. Mp 47–49 °C (lit.,[27] 48–51 °C); $\delta_H$ 6.84 (s, 4H), 4.09–4.06 (m, 4H), 3.84–3.81 (m, 4H), 3.73–3.66 (m, 12H), 3.62–3.59 (m, 4H) and 2.50 (t, 2H) (see also Table 5); $\delta_C$ 153.1, 115.6, 72.4, 70.8, 70.4, 69.8, 68.0 and 61.7; $\nu_{max}$(FTIR, KBr)/cm$^{-1}$ 3250 (broad), 1232, 1118, 1067.

**1,4-Bis(1-benzoyloxy-3,6,9-trioxanonyl)benzene (8).** To a solution of **1d** (0.68 g, 1.8 mmol) in 1,2-dichloromethane (20 ml) was added successively benzoyl chloride (0.52 g, 3.7 mmol) and freshly distilled dry pyridine (2 ml, 25 mmol). The reaction mixture was heated at reflux temperature for 2 h, cooled to room temperature and washed three times with water (25 ml). The organic layer was dried on magnesium sulfate and the filtrate was concentrated under reduced pressure to yield 0.70 g (1.20 mmol, 66%) of pure **8** as a waxy solid. $\delta_H$ 8.05 (dd, 4H, $J$ 1.5 and 8.3), 7.54 (m, 2H), 7.41 (m, 4H), 6.80 (s, 4H), 4.49–4.46 (m, 4H), 4.05–4.02 (m, 4H), 3.86–3.80 (m, 8H) and 3.72 (s, 8H); $\delta_C$ 166.5, 153.1, 133.0, 130.1, 129.7, 128.3, 115.6, 70.8, 70.8, 69.9, 69.3, 68.1 and 64.1.

**Bis(1-phenoxy-3,6,9-trioxanonyl) terephthalate (9).** To a solution of (9-hydroxy-1,4,7-trioxanonyl)benzene (0.70 g, 3.1 mmol) {prepared according to the procedure of **1b**–**d** from phenol, 2-[2-(2-ethoxy)ethoxy]ethanol and potassium carbonate in DMF} in dichloromethane (20 ml) was added successively terephthaloyl dichloride (0.31 g, 1.53 mmol) and freshly distilled dry pyridine (2 ml, 25 mmol). The reaction mixture was heated at reflux temperature for 2 h, cooled to room temperature and washed three times with water (25 ml) containing NaCl. The organic layer was dried on magnesium sulfate and the filtrate was concentrated under reduced pressure to yield 0.74 g (1.27 mmol, 83%) of pure **9** as a waxy solid. $\delta_H$ 8.10 (s, 4H), 7.29–7.24 (m, 4H), 6.96–6.87 (m, 6H), 4.52–4.48 (m, 4H), 4.12–4.09 (m, 4H), 3.87–3.84 (m, 8H) and 3.76 (s, 8H); $\delta_C$ 165.7, 158.6, 133.8, 129.6, 129.4, 120.8, 114.5, 70.8, 70.7, 69.8, 69.1, 67.2 and 64.5.

**General procedure for solution condensation polymerization.** The appropriate diol (10.0 mmol) was dissolved in either 300 ml (monomer conc. 0.033 M) or 30 ml (monomer conc. 0.33 M) of 1,2-dichloroethane. After the solution was deareated and placed under a dry nitrogen atmosphere the appropriate bis-acid chloride (10.0 mmol) was added. Subsequently, pyridine (5 ml) was added dropwise to the reaction mixture at room temperature. After heating at reflux temperature for 3 h, the reaction mixture was cooled to room temperature, concentrated under reduced pressure to one-third of its volume and poured into a five-fold excess of vigorously stirred methanol. The methanol solution was decanted from the oily precipitate and concentrated under reduced pressure to yield a light brown oil containing the cyclic oligomers. The cyclic oligomers were isolated using preparative column chromatography [silica; eluent acetone–*n*-hexane (1 : 1 v/v)]. The purity of all cyclic oligomers was established using HPLC.

**General procedure for melt condensation polymerization.**[1] Equimolar amounts (5.0 mmol) of the diol and the bis-acid chloride were mixed in a Schlenk flask (25 ml) under a nitrogen atmosphere and subsequently heated at 100 °C under magnetic stirring. To remove the evolving HCl gas the Schlenk flask was

continuously flushed with a stream of nitrogen gas. After 20–30 min at 100 °C stirring became impaired due to an increase in viscosity of the reaction mixture. Therefore, the reaction mixture was gradually heated from 100–180 °C in 20 min in order to force the reaction to completion. After cooling to room temperature the reaction mixture was dissolved in THF (30 ml) and the polymer was precipitated in a five-fold excess of vigorously stirred methanol. The methanol solution was decanted from the oily precipitate and concentrated under reduced pressure yielding a light brown oil containing the series of cyclic oligomers.

3,6,9,12,23,26,29,32-*Octaoxatetracyclo*[32.2.2.$0^{13,18}$.$0^{17,22}$]-*octatriaconta*-1(36),13,15,17(22),18,20,34,37-*octaene*-2,33-*dione* [**3a**(1)].—0.57 g (1.03 mmol, 10.3%) of a white solid. Mp 117–118 °C; DSC 116.7 °C, Δ*H* 26.8 cal $g^{-1}$; $\delta_H$ 7.79 (d, 2H, *J* 8.6), 7.64 (s, 4H), 7.23 (dd, 2H, *J* 8.6 and 7.6), 6.71 (d, 2H, *J* 7.6), 4.47–4.44 (m, 4H), 4.21–4.18 (m, 4H), 4.00–3.98 (m, 4H), 3.88–3.80 (m, 8H) and 3.77–3.75 (m, 4H); $\delta_C$ 165.7, 154.2, 133.3, 129.1, 126.7, 124.9, 114.6, 105.6, 71.1, 70.9, 69.7, 69.1, 68.0 and 64.2; $\nu_{max}$(FTIR, KBr)/$cm^{-1}$ 1721, 1271, 1097; *m*/*z* (FABMS) 555 ($[M+H]^+$); (Calc. for $C_{30}H_{34}O_{10}$: C, 64.97; H, 6.18; O, 28.85. Found: C, 64.86; H, 6.19%).

3,6,9,12,23,26,29,32,39,42,45,48,59,62,65,68-*Hexadecaoxaheptacyclo*[68.2.2.$2^{34,37}$.$0^{13,18}$.$0^{17,22}$.$0^{49,54}$.$0^{53,58}$]*hexaheptaconta*-1(72),13,15,17,19,21,34,36,49,51,53,55,57,70,73,75-*hexadecaene*-2,33,38,69-*tetraone* [**3a**(2)].—0.18 g (0.16 mmol, 3.2%) of a white solid. Mp 125–126 °C; DSC 125.0 °C, Δ*H* 17.1 cal $g^{-1}$; $\delta_H$ 7.99 (s, 8H), 7.81 (d, 4H, *J* 8.4), 7.27 (dd, 4H, *J* 8.4 and 7.6), 6.76 (d, 4H, *J* 7.6), 4.48–4.45 (m, 8H), 4.23–4.20 (m, 8H), 3.97–3.94 (m, 8H) and 3.84–3.71 (m, 24H); $\delta_C$ 165.7, 154.3, 133.8, 129.5, 126.7, 125.0, 114.5, 105.6, 71.0, 70.9, 69.8, 69.1, 67.9 and 64.5; $\nu_{max}$(FTIR, KBr)/$cm^{-1}$ 1726, 1272, 1099; *m*/*z* (FABMS) 1109 ($[M+H]^+$); (Calc. for $C_{60}H_{68}O_{20}$: C, 64.97; H, 6.18; O, 28.85. Found: C, 64.92; H, 6.21%).

3,6,9,12,23,26,29,32,39,42,45,48,59,62,65,68,75,78,81,84,95,98,101,104-*Tetracosaoxadecacyclo*[104.2.2.2$^{34,37}$.2$^{70,73}$.$0^{13,18}$.$0^{17,22}$.$0^{49,54}$.$0^{53,58}$.$0^{85,90}$.$0^{89,94}$]*tetradecaundeca*-1(108),13,15,17,19,21,34,36,49,51,53,55,57,70,72,85,87,89,91,93,106,109,111,113-*tetracosaene*-2,33,38,69,74,105-*hexaone* [**3a**(3)].—0.069 g (0.04 mmol, 1.2%) of a colourless oil. $\delta_H$ 8.03 (s, 12H), 7.82 (d, 6H, *J* 8.5), 7.29 (dd, 6H, *J* 8.5 and 7.6), 6.77 (d, 6H, *J* 7.6), 4.48–4.45 (m, 12H), 4.24–4.21 (m, 12H), 3.97–3.93 (m, 12H) and 3.85–3.71 (m, 36H); $\delta_C$ 165.6, 154.2, 133.8, 129.5, 126.7, 125.0, 114.5, 105.6, 70.9, 70.8, 69.8, 69.1, 67.8 and 64.5; *m*/*z* (FABMS) 1663 ($[M+H]^+$); (Calc. for $C_{90}H_{102}O_{30}$: C, 64.97; H, 6.18; O, 28.85. Found: C, 64.89; H, 6.22%).

3,6,9,12,23,26,29,32,39,42,45,48,59,62,65,68,75,78,81,84,95,98,101,104,111,114,117,120,131,134,137,140-*Dotriacontaoxatridecacyclo*[140.2.2.2$^{34,37}$.2$^{70,73}$.2$^{106,109}$.$0^{13,18}$.$0^{17,22}$.$0^{49,54}$.$0^{53,58}$.$0^{85,90}$.$0^{89,94}$.$0^{121,126}$.$0^{125,130}$]*dopentacontahecta*-1(144),13,15,17,19,21,34,36,49,51,53,55,57,70,72,85,87,89,91,93,106,108,121,123,125,127,129,142,144,145,147,149,151-*dotriacontaene*-2,33,38,69,74,105,110,141-*octaone* [**3a**(4)].—0.068 g (0.03 mmol, 1.2%) of a light yellow oil. $\delta_H$ 8.04 (s, 16H), 7.82 (d, 8H, *J* 8.5), 7.29 (dd, 8H, *J* 8.5 and 7.6), 6.79 (d, 8H, *J* 7.6), 4.48–4.45 (m, 16H), 4.23–4.21 (m, 16H), 3.99–3.94 (m, 16H) and 3.85–3.72 (m, 48H); $\delta_C$ 165.7, 154.3, 133.8, 129.6, 126.7, 125.0, 114.6, 105.7, 71.0, 70.8, 69.8, 69.1, 67.9 and 64.5; *m*/*z* (FABMS) 2217 ($[M+H]^+$); (Calc. for $C_{120}H_{136}O_{40}$: C, 64.97; H, 6.18; O, 28.85. Found: C, 64.94; H, 6.24%).

3,6,9,12,23,26,29,32,39,42,45,48,59,62,68,75,78,81,84,95,98,101,104,111,114,117,120,131,134,137,140,147,150,153,156,167,170,173,176-*Tetracontaoxahexadecacyclo*[176.2.2.2$^{34,37}$.2$^{70,73}$.2$^{106,109}$.2$^{142,145}$.$0^{13,18}$.$0^{17,22}$.$0^{49,54}$.$0^{53,58}$.$0^{85,90}$.$0^{89,94}$.$0^{121,126}$.$0^{125,130}$.$0^{157,162}$.$0^{161,166}$]*nonacontahecta*-1(180),13,15,17,19,21,34,36,49,51,53,55,57,70,72,85,87,89,91,93,106,108,121,123,125,127,129,142,144,157,159,161,163,165,178,181,183,185,187,189-*tetracontaene*-2,33,38,69,74,105,110,141,146,177-*decaone* [**3a**(5)].—0.008 g (0.003 mmol, 0.1%) of a light yellow oil. $\delta_H$ 8.05 (s, 20H), 7.82 (d, 10H, *J* 8.5), 7.29 (dd, 10H, *J* 8.5 and 7.6), 6.77 (d, 10H, *J* 7.6), 4.48–4.45 (m, 20H), 4.25–4.22 (m, 20H), 3.97–3.94 (m, 20H) and 3.85–3.71 (m, 60H); $\delta_C$ 165.7, 154.3, 133.8, 129.6, 126.7, 125.0, 114.6, 105.7, 71.0, 70.8, 69.8, 69.1, 67.9 and 64.5; *m*/*z* (FABMS) 2771 ($[M+H]^+$).

3,6,9,12,19,22,25,28-*Octaoxatricyclo*[28.2.2.$0^{13,18}$]*tetratriaconta*-1(32),13(18),14,16,30,33-*hexaene*-2,29-*dione* [**3b**(1)].—1.12 g (3.0 mmol, 30%) of a white solid. Mp 81–82 °C; DSC 80.7 °C, Δ*H* 23.0 cal $g^{-1}$; $\delta_H$ 8.07 (s, 4H), 6.94–6.85 (m, 4H), 4.50–4.47 (m, 4H), 4.13–4.09 (m, 4H), 3.85–3.79 (m, 8H) and 3.72 (s, 8H); $\delta_C$ 165.6, 149.1, 133.9, 129.6, 121.8, 115.9, 71.0, 70.8, 69.9, 69.0 and 64.7; $\nu_{max}$(FTIR, KBr)/$cm^{-1}$ 1737, 1282, 1140; *m*/*z* (FABMS) 505 ($[M+H]^+$); (Calc. for $C_{26}H_{32}O_{10}$: C, 61.90; H, 6.39; O, 31.71. Found: C, 61.78; H, 6.42; O, 31.66%).

3,6,9,12,19,22,25,28,35,38,41,44,51,54,57,60-*Hexadecaoxapentacyclo*[60.2.2.2$^{30,33}$.$0^{13,18}$.$0^{45,50}$]*octahexaconta*-1(64),13,15,17,30,32,45(50),46,48,62,65,67-*dodecaene*-2,29,34,61-*tetraone* [**3b**(2)].—0.19 g (0.25 mmol, 5%) of a white solid. Mp 113–115 °C; DSC 111.1 °C, Δ*H* 18.0 cal $g^{-1}$; $\delta_H$ 8.05 (s, 8H), 6.87 (s, 8H), 4.48–4.45 (m, 8H), 4.13–4.10 (m, 8H), 3.85–3.81 (m, 16H) and 3.76–3.67 (m, 16H); $\delta_C$ 165.6, 149.0, 133.8, 129.5, 121.6, 114.8, 70.8, 70.7, 69.8, 69.1, 68.9 and 64.5; $\nu_{max}$(FTIR, KBr)/$cm^{-1}$ 1730, 1271, 1128; *m*/*z* (FABMS) 1009 ($[M+H]^+$); (Calc. for $C_{52}H_{64}O_{20}$: C, 61.90; H, 6.39; O, 31.71. Found: C, 61.30; H, 6.34%).

3,6,9,12,19,22,25,28,35,38,41,44,51,54,57,60,67,70,73,76,83,86,89,92-*Tetracosaoxaheptacyclo*[92.2.2.2$^{30,33}$.2$^{62,65}$.$0^{13,18}$.$0^{45,50}$.$0^{77,82}$]*dohecta*-1(96),13,15,17,30,32,45,47,49,62,64,77,79,81,94,96,97,99,101-*octadecaene*-2,29,34,61,66,93-*hexaone* [**3b**(3)].—0.04 g (0.03 mmol, 1%) of a colourless oil. $\delta_H$ 8.05 (s, 12H), 6.87 (s, 12H), 4.48–4.45 (m, 12H), 4.13–4.10 (m, 12H), 3.85–3.80 (m, 24H) and 3.75–3.67 (m, 24H); $\delta_C$ 165.6, 148.9, 133.8, 129.5, 121.6, 114.8, 70.8, 70.7, 69.8, 69.0, 68.8 and 64.4; *m*/*z* (FABMS) 1513 ($[M+H]^+$).

3,6,9,12,18,21,24,27-*Octaoxatricyclo*[27.2.2.1$^{13,17}$]*tetratriaconta*-1(31),13,15,17(34),29,32-*hexaene*-2,28-*dione* [**3c**(1)].—0.79 g (2.1 mmol, 21%) of a white solid. Mp 98–99 °C; DSC 98.6 °C, Δ*H* 23.8 cal $g^{-1}$; $\delta_H$ 8.06 (s, 4H), 7.12 (t, 1H, *J* 8.2), 6.48 (dd, 2H, *J* 8.2 and 2.3), 6.37 (t, 1H, *J* 2.3), 4.52–4.49 (m, 4H), 4.02–3.99 (m, 4H), 3.86–3.83 (m, 8H) and 3.77–3.72 (m, 8H); $\delta_C$ 165.7, 159.8, 133.8, 129.7, 129.6, 107.1, 101.1, 71.1, 70.7, 69.7, 69.1, 67.4 and 64.6; $\nu_{max}$(FTIR, KBr)/$cm^{-1}$ 1739, 1726, 1270, 1119; *m*/*z* (FABMS) 505 ($[M+H]^+$); (Calc. for $C_{26}H_{32}O_{10}$: C, 61.90; H, 6.39; O, 31.71. Found: C, 62.03; H, 6.38; O, 31.64%).

3,6,9,12,18,21,24,27,34,37,40,43,49,52,55,58-*Hexadecaoxapentacyclo*[58.2.2.2$^{29,32}$.1$^{13,17}$.1$^{44,48}$]*octahexaconta*-1(62),13,15,17(68),29,31,45,47,60,63,65,67-*dodecaene*-2,28,33,59-*tetraone* [**3c**(2)].—0.11 g (0.15 mmol, 3%) of a white solid. Mp 73–74 °C; DSC 74.2 °C, Δ*H* 11.1 cal $g^{-1}$; $\delta_H$ 8.07 (s, 8H), 7.12 (m, 2H), 6.48–6.45 (m, 6H), 4.50–4.47 (m, 8H), 4.07–4.04 (m, 8H), 3.86–3.80 (m, 16H) and 3.72 (s, 16H); $\delta_C$ 165.7, 159.9, 133.9, 129.8, 129.6, 107.1, 101.8, 70.8, 69.8, 69.1, 67.4 and 64.5; $\nu_{max}$(FTIR, KBr)/$cm^{-1}$ 1733, 1266, 1095; *m*/*z* (FABMS) 1009 ($[M+H]^+$); (Calc. for $C_{52}H_{64}O_{20}$: C, 61.90; H, 6.39; O, 31.71. Found: C, 61.98; H, 6.43%).

2,5,8,11,18,21,24,27-*Octaoxatricyclo*[26.2.2.2$^{13,16}$]*tetratriaconta*-1(30),13,15,28,31,33-*hexaene*-12,17-*dione* [**3d**(1)].—0.86 g (2.3 mmol, 23%) of a white solid. Mp 91–92 °C; DSC 91.6 °C, Δ*H* 18.3 cal $g^{-1}$; $\delta_H$ 8.03 (s, 4H), 6.71 (s, 4H), 4.53–4.49 (m, 4H), 3.99–3.96 (m, 4H), 3.88–3.85 (m, 4H), 3.81–3.78 (m, 4H) and 3.72 (s, 8H); $\delta_C$ 165.7, 153.1, 133.9, 129.5, 115.8, 70.9, 70.8, 69.7, 69.0, 68.4 and 64.3; $\nu_{max}$(FTIR, KBr)/$cm^{-1}$ 1717, 1279, 1116; *m*/*z* (FABMS) 505 ($[M+H]^+$); (Calc. for $C_{26}H_{32}O_{10}$: C, 61.90; H, 6.39; O, 31.71. Found: C, 61.86; H, 6.46%).

2,5,8,11,18,21,24,27,32,35,38,41,48,51,54,57-*Hexadecaoxapentacyclo*[56.2.2.2$^{13,16}$.2$^{28,31}$.2$^{43,46}$]*octahexaconta*-1(60),13,15,28,30,43,49,58,61,63,65,67-*dodecaene*-12,17,42,47-*tetraone* [**3d**(2)].—0.15 g (0.20 mmol, 4%) of a white solid. Mp 113–115 °C; DSC 115.3 °C, Δ*H* 23.6 cal $g^{-1}$; $\delta_H$ 8.07 (s, 8H), 6.80 (s, 8H), 4.50–4.47 (m, 8H), 4.02–3.99 (m, 8H), 3.85–3.78 (m, 16H)

and 3.71 (s, 16H); $\delta_H$ 165.7, 153.0, 133.9, 129.6, 115.5, 70.8 (2×), 69.9, 69.1, 68.0 and 64.5; $\nu_{max}$(FTIR, KBr)/cm$^{-1}$ 1721, 1279, 1114; *m/z* (FABMS) 1009 ([M+H]$^+$); (Calc. for $C_{52}H_{64}O_{20}$: C, 61.90; H, 6.39; O, 31.71. Found: C, 61.78; H, 6.34%).

2,5,8,11,18,21,24,27,32,35,38,41,48,51,54,57,62,65,68,71,78,81,84,87-*Tetracosaoxaheptacyclo*[86.2.2.2$^{13,16}$.2$^{28,31}$.2$^{43,46}$.2$^{58,61}$.2$^{73,76}$]*dohecta*-1(90),13,15,28,30,43,45,58,60,73,75,88,91,93,95,97,99,101-*octadecaene*-12,17,42,47,72,77-*hexaone* [**3d**(3)].—0.04 g (0.025 mmol, 1%) of a colourless oil. $\delta_H$ 8.07 (s, 12H), 6.78 (s, 12H), 4.48–4.45 (m, 12H), 4.02–3.99 (m, 12H), 3.84–3.78 (m, 24H) and 3.70 (s, 24H); $\delta_C$ 165.6, 153.0, 133.9, 129.5, 115.5, 70.7 (2×), 69.8, 69.1, 68.0 and 64.5; *m/z* (FABMS) 1513 ([M+H]$^+$).

6,9,12,15,22,25,28,31-*Octaoxatricyclo*[30.4.0.0$^{5,36}$]*hexatriaconta*-1,3,5(36),32,34-*pentaene*-16,21-*dione* [**6a**(1)].—0.86 g (1.61 mmol, 16.4%) of colourless crystals. Mp 96–98 °C; DSC 100.7 °C, $\Delta H$ 33.7 cal g$^{-1}$; $\delta_H$ 7.87 (d, 2H, *J* 8.5), 7.34 (dd, 2H, *J* 8.5 and 7.6), 6.87 (d, 2H, *J* 7.6), 4.33–4.30 (m, 4H), 4.13–4.10 (m, 4H), 4.01–3.98 (m, 4H), 3.79–3.77 (m, 4H), 3.68–3.64 (m, 8H), 2.01–1.94 (m, 4H) and 1.32–1.27 (m, 4H); $\delta_C$ 173.2, 154.3, 126.9, 125.1, 114.6, 105.9, 71.0, 70.8, 69.8, 69.0, 68.2, 63.3, 33.5 and 24.0; $\nu_{max}$(FTIR, KBr)/cm$^{-1}$ 1746, 1730, 1265, 1159; *m/z* (FABMS) 535 ([M+H]$^+$); (Calc. for $C_{28}H_{38}O_{10}$: C, 62.91; H, 7.17; O, 29.92. Found: C, 62.74; H, 7.15%).

6,9,12,15,22,25,28,31,42,45,48,51,58,61,64,67-*Hexadecaoxapentacyclo*[66.4.0.0$^{5,72}$.0$^{32,37}$.0$^{36,41}$]*henheptaconta*-1,3,5(72),32,34,36(41),37,39,68,70-*decaene*-16,21,52,57-*tetraone* [**6a**(2)].—0.26 g (0.24 mmol, 4.9%) of a light brown solid. Mp 52–53 °C; DSC 52.5 °C, $\Delta H$ 18.1 cal g$^{-1}$; $\delta_H$ 7.85 (d, 4H, *J* 8.5), 7.32 (dd, 4H, *J* 8.5 and 7.6), 6.82 (d, 4H, *J* 7.6), 4.30–4.25 (m, 8H), 4.23–4.18 (m, 8H), 4.00–3.94 (m, 8H), 3.81–3.74 (m, 8H), 3.73–3.64 (m, 16H), 2.30–2.25 (m, 8H), 1.62–1.57 (m, 8H); $\delta_C$ 173.2, 154.3, 126.8, 125.1, 114.6, 105.7, 70.9, 70.7, 69.8, 69.2, 67.9, 63.5, 33.7, 24.2; $\nu_{max}$(FTIR, KBr)/cm$^{-1}$ 1738, 1269, 1165; *m/z* (FABMS) 1069 ([M+H]$^+$); (Calc. for $C_{56}H_{76}O_{20}$: C, 62.91; H, 7.17; O, 29.92. Found: C, 62.81; H, 7.19%).

3,6,9,12,23,26,29,32-*Octaoxatetracyclo*[32.3.1.0$^{13,18}$.0$^{17,22}$]*octatriaconta*-1(38),13,15,17(22),18,20,34,36-*octaene*-2,33-*dione* [**6b**(1)].—1.08 g (1.95 mmol, 19.5%) of a white solid. Mp 81–82 °C; DSC 82.2 °C, $\Delta H$ 15.2 cal g$^{-1}$; $\delta_H$ 8.46 (t, 1H, *J* 1.5), 7.86 (dd, 2H, *J* 7.8 and 1.5), 7.71 (d, 2H, *J* 8.5), 7.16 (dd, 2H, *J* 8.5 and 7.6), 6.94 (t, 1H, *J* 7.8), 6.69 (d, 2H, *J* 7.6), 4.36–4.32 (m, 4H), 4.24–4.21 (m, 4H), 3.98–3.95 (m, 4H), 3.81–3.78 (m, 8H) and 3.74–3.71 (m, 4H); $\delta_C$ 165.5, 154.2, 133.3, 130.7, 130.1, 128.1, 126.7, 124.8, 114.5, 105.8, 71.1, 71.0, 69.8, 69.0, 68.0 and 64.2; $\nu_{max}$(FTIR, KBr)/cm$^{-1}$ 1724, 1258, 1109; *m/z* (FABMS) 555 ([M+H]$^+$); (Calc. for $C_{30}H_{34}O_{10}$: C, 64.97; H, 6.18; O, 28.85. Found: C, 65.11; H, 6.22; O, 28.74%).

3,6,9,12,23,26,29,32,40,43,46,49,60,63,66,69-*Hexadecaoxaheptacyclo*[69.3.1.1$^{34,38}$.0$^{13,18}$.0$^{17,22}$.0$^{50,55}$.0$^{54,59}$]*hexaheptaconta*-1(75),13,15,17(22),18,20,34,36,38(76),50(55),51,53,56,58,71,73-*hexadecaene*-2,33,39,70-*tetraone* [**6b**(2)].—0.27 g (0.24 mmol, 4.8%) of a white solid. Mp 120–121 °C; DSC 120.5 °C, $\Delta H$ 22.8 cal g$^{-1}$; $\delta_H$ 8.66 (t, 2H, *J* 1.5), 8.15 (dd, 4H, *J* 7.8 and 1.7), 7.79 (d, 4H, *J* 8.5), 7.38 (t, 2H, *J* 7.8), 7.25 (dd, 4H, *J* 8.5 and 7.6), 6.73 (d, 4H, *J* 7.6), 4.46–4.43 (m, 8H), 4.22–4.19 (m, 8H), 3.96–3.93 (m, 8H), 3.84–3.76 (m, 16H) and 3.73–3.70 (m, 8H); $\delta_C$ 165.7, 154.3, 133.9, 130.8, 130.5, 128.5, 126.7, 125.0, 114.6, 105.7, 71.0, 70.8, 69.8, 69.2, 67.9 and 64.5; $\nu_{max}$(FTIR, KBr)/cm$^{-1}$ 1732, 1253, 1082; *m/z* (FABMS) 1109 ([M+H]$^+$); (Calc. for $C_{60}H_{68}O_{20}$: C, 64.97; H, 6.18; O, 28.85. Found: C, 64.90; H, 6.25%).

**Polymer Fraction.** *Polymer* **4a**.—Precipitation of the crude product in methanol gave 1.80 g (65%) of a light brown viscous oil. $\delta_H$([$^2$H$_6$]DMSO) 7.97 (s, 4H), 6.67–7.65 (m, 2H), 7.31–7.25 (m, 2H), 6.86 (m, 2H), 4.37 (m, 4H), 4.14 (m, 4H), 3.82–3.74 (m, 8H) and 3.62 (s, 8H); $\delta_C$([$^2$H$_6$]DMSO) 164.8, 153.7, 133.4, 129.3, 125.9, 125.2, 113.7, 105.8, 70.0, 69.9, 68.9, 68.2, 67.6 and 64.4; GPC $M_r$ 1.8 × 10$^4$, *D* 1.80; DSC $T_g$ 9.3 °C (midpoint).

*Polymer* **4b**.—Precipitation afforded 1.36 g (54%) of a brown viscous oil. $\delta_H$([$^2$H$_6$]DMSO) 8.03 (m, 4H), 6.89–6.83 (m, 4H), 4.38 (m, 4H), 4.40 (m, 4H), 3.73–3.68 (m, 8H), 3.58 (s, 8H); $\delta_C$([$^2$H$_6$]DMSO) 165.4, 148.3, 133.5, 129.4, 121.1, 114.3, 69.9 (2×), 69.0, 68.2 (2×) and 64.4; GPC $M_r$ 5 × 10$^3$, *D* 1.48; DSC $T_g$ −14.2 °C (midpoint).

*Polymer* **4c**.—Precipitation of the crude product in methanol gave 1.31 g (52%) of a viscous brown oil. $\delta_H$([$^2$H$_6$]DMSO) 8.04 (s, 4H), 7.10 (m, 1H), 6.50–6.44 (m, 3H), 4.41 (m, 4H), 3.93 (m, 4H), 3.76–3.69 (m, 8H) and 3.60 (s, 8H); $\delta_C$([$^2$H$_6$]DMSO) 165.7, 159.9, 133.9, 129.6, 107.1, 101.8, 70.9, 70.7, 69.8, 69.2, 67.4 and 64.5; GPC $M_r$ 5 × 10$^3$, *D* 1.50; DSC $T_g$ −17.8 °C (midpoint).

*Polymer* **4d**.—Precipitation of the crude product afforded 1.46 g (58%) of a light brown viscous oil. $\delta_H$([$^2$H$_6$]DMSO) 8.04 (s, 4H), 6.77 (s, 4H), 4.42–4.40 (m, 4H), 3.94–3.91 (m, 4H), 3.76–3.74 (m, 4H), 3.68–3.65 (m, 4H) and 3.58 (s, 8H); $\delta_C$([$^2$H$_6$]DMSO) 164.8, 152.4, 133.4, 129.3, 115.1, 69.7, 68.9, 68.1, 67.3 and 64.3; GPC $M_r$ 2.6 × 10$^4$, *D* 1.89; DSC $T_g$ −5.7 °C (midpoint).

## Acknowledgements

Experimental contributions by R. H. G. Neilen and M. J. J. Mulder are gratefully acknowledged. This work was supported in part (A. L. S., N. V. and W. J. J. S.) by the Netherlands Foundation of Chemical Research (SON) with financial aid from the Netherlands Organization for Scientific Research (NWO).

## References

1 M. Ballauf, *Makromol. Chem., Rapid Commun.*, 1986, **7**, 409.
2 V. Percec, C. Pugh, O. Nuyken and S. D. Pask, in *Comprehensive Polymer Science*, ed. G. Allen and J. C. Bevington, Pergamon Press, Oxford, 1989, vol. 6, p. 281.
3 R. Hilgenfeld and W. Saenger, *Topics Curr. Chem.*, 1982, **101**, 1; F. Vögtle, *Supramolekulare Chemie*, B. G. Teubner, Stuttgart, 1989; B. Dietrich, P. Viout and J.-M. Lehn, *Macrocyclic Compounds Chemistry*, VCH Thieme, Weinheim, 1992.
4 F. Vögtle, S. Meier and R. Hoss, *Angew. Chem., Int. Ed. Engl.*, 1992, **31**, 1619 and references cited therein.
5 H. M. Colquhoun, C. C. Dudman, M. Thomas, C. A. O'Mahony and D. J. Williams, *J. Chem. Soc., Chem. Commun.*, 1990, 336; V. Percec, M. Kawasumi, P. L. Rinaldi, V. E. Litman, *Macromolecules*, 1992, **25**, 3851; W. Memeger, J. Lazar, Jr., D. Ovenall, A. J. Arduengo and R. A. Leach, *Macromol. Symp.*, 1994, **77**, 105; D. J. Brunelle, H. O. Krabbenhoft and D. K. Bonauto, *Macromol. Symp.*, 1994, **77**, 117; B. R. Wood, J A. Semleyn and P. Hodge, *Polymer*, 1994, **35**, 1542; M. Rothe, M. Lohmüller, U. Breuksch and G. Schmidtberg, *Angew. Chem., Int. Ed. Engl.*, 1994, **33**, 1960 and references cited therein.
6 F. J. Carver, C. A. Hunter and R. J. Shannon, *J. Chem. Soc., Chem. Commun.*, 1994, 1277.
7 T. Ogawa, A. Yoshikawa, H. Wada, C. Ogawa, N. Ono and H. Suzuki, *J. Chem. Soc., Chem. Commun.*, 1995, 1407.
8 B. H. Kim, E. J. Jeong and W. H. Jung, *J. Am. Chem. Soc.*, 1995, **117**, 6390.
9 S. Inokuma, S. Sakai and J. Nishimura, *Top. Curr. Chem.*, 1994, **172**, 87 and references cited therein.
10 For **3a**(*n*) with *n* = 1–5 preliminary communication: I. J. A. Mertens, L. W. Jenneskens, E. J. Vlietstra, A. C. Van der Kerk-van Hoof, J. W. Zwikker, W. J. J. Smeets and A. L. Spek, *J. Chem. Soc., Chem. Commun.*, 1995, 1621 and references cited therein.
11 D. A. Jaeger and R. R. Whitney, *J. Org. Chem.*, 1975, **40**, 92.
12 R. T. Gray, D. N. Reinhoudt, K. Spaargaren and J. F. De Bruijn, *J. Chem. Soc., Perkin Trans. 2*, 1977, 206.
13 N. J. Turro, *Modern Molecular Photochemistry*, Benjamin/Cummings, London, 1978.
14 WIN-NMR Bruker Spectrospin AG Fällanden, Switzerland, 1990; P. Budzelaar, GeNMR (version 3.51), IvorySoft, Amsterdam, The Netherlands, 1994.
15 R. Abraham and G. Gatti, *J. Chem. Soc. B*, 1969, 961; L. Philips and V. Wray, *J. Chem. Soc., Perkin Trans. 2*, 1972, 536 and references cited therein; J. Dale, *Tetrahedron*, 1974, **30**, 1683; E. Riande, M. Jimeno, R. Salvador, J. De Abajo and J. Guzman, *J. Phys. Chem.*, 1990, **94**, 7435.

16 MMX force field as implemented in PCMODEL 4.0, Serena Software, Bloomington, IN, USA, 1990; AM1: M. J. S. Dewar, E. G. Zoebisch, E. F. Healy and J. J. P. Stewart, *J. Am. Chem. Soc.*, 1985, **107**, 3902; MOPAC 7.0: J. J. P. Stewart, 1993.
17 *CRC Handbook of Chemistry and Physics*, ed. D. R. Lide, CRC Press, Boca Raton, 76th edn., 1995–1996.
18 J. Liptay and W. Liptay, *Z. Naturforsch.*, *Teil A*, 1960, **20a**, 1441.
19 J. March, *Advanced Organic Chemistry*, *Reactions*, *Mechanisms and Structure*, Wiley, New York, 4th edn., 1992.
20 D. B. Amabilino and J. F. Stoddart, *Chem. Rev.*, 1995, **95**, 2725 and references cited therein; P. R. Ashton, J. Huff, S. Menzer, I. W. Parsons, J A. Preece, J. F. Stoddart, M. S. Tolley, A. J. P. White and D. J. Williams, *Chem. Eur. J.*, 1996, **2**, 31 and references cited therein.
21 C. A. Hunter, *Chem. Soc. Rev.*, 1994, 101 and references cited therein.
22 I. J. A. Mertens, J. E. M. J. Raaymakers, L. W. Jenneskens and A. L. Spek, *QCPE Bulletin*, 1995, **15**, 30.
23 E. Weber, J. L. Toner, I. Goldberg, F. Vögtle, D. A. Laidler, J. F. Stoddart, R. A. Bartsch and C. L. Liotta, in *Crown Ethers and Analogs*, ed. S. Patai and Z. Rappoport, Wiley, Chichester, 1989, p. 402.
24 G. M. Sheldrick, SHELXS-86. Program for crystal structure determination, Univ. of Göttingen, Federal Republic of Germany, 1986.
25 G. M. Sheldrick, SHELXL-93. Program for crystal structure refinement, Univ. of Göttingen, Federal Republic of Germany, 1993.
26 S. Shinkai, K. Inuzuka, O. Miyazaki and O. Manabe, *J. Am. Chem. Soc.*, 1985, **107**, 3950.
27 P. L. Anelli, P. R. Ashton, N. Spencer, A. M. Z. Slawin, J. Fraser Stoddart and D. J. Williams, *Angew. Chem.*, *Int. Ed. Engl.*, 1991, **30**, 1036.
28 M. J. Gunter, D. C. R. Hockless, M. R. Johnston, B. W. Skelton and A. H. White, *J. Am. Chem. Soc.*, 1994, **116**, 4810.

*Paper* 7/01920C
*Received* 19*th March* 1997
*Accepted* 29*th October* 1997